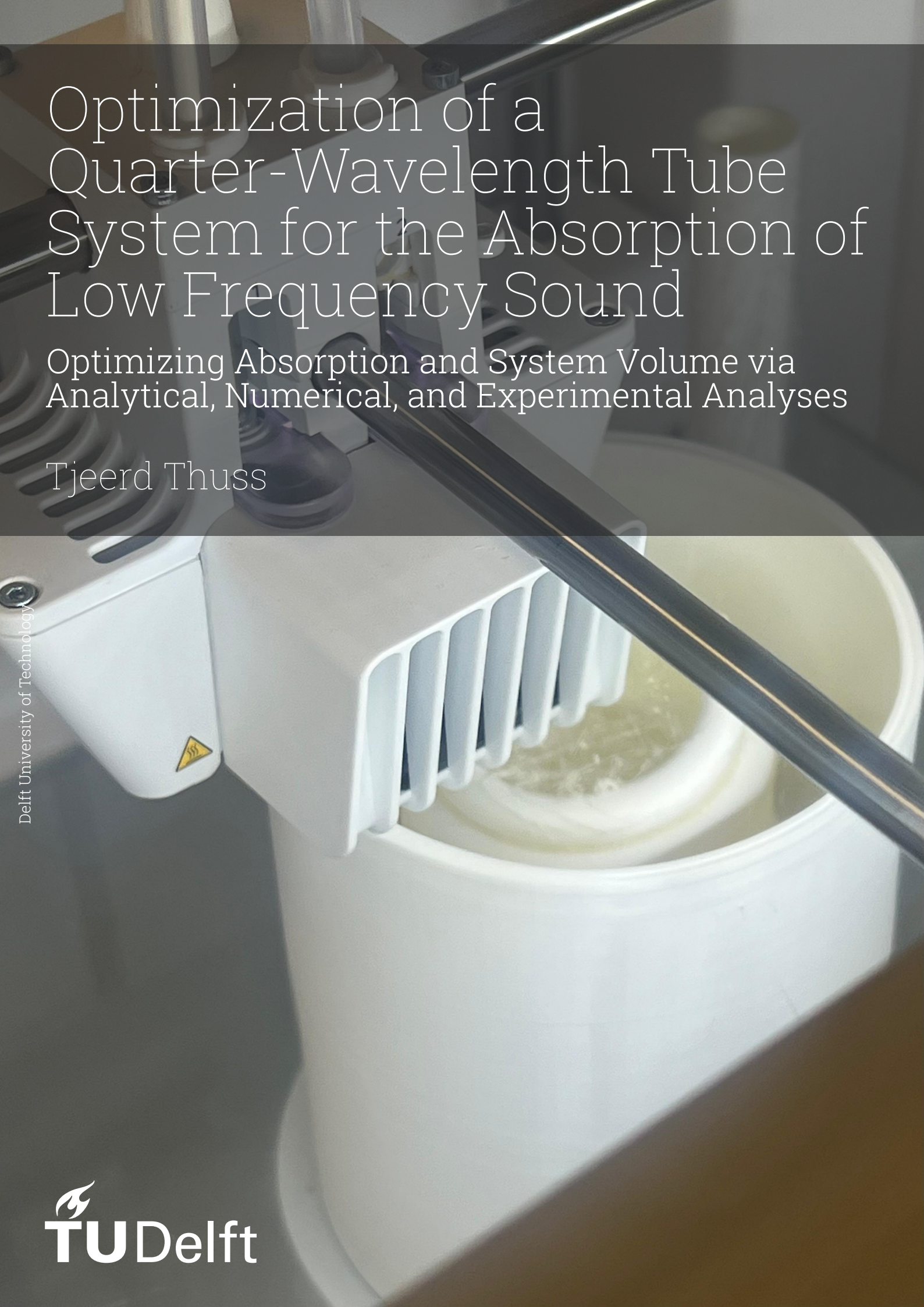

Optimization of a Quarter-Wavelength Tube System for the Absorption of Low Frequency Sound

Optimizing Absorption and System Volume via Analytical, Numerical, and Experimental Analyses

Tjeerd Thuss

Delft University of Technology

TU Delft

Optimization of a Quarter-Wavelength Tube System for the Absorption of Low Frequency Sound

Optimizing Absorption and System Volume via Analytical, Numerical, and Experimental Analyses

by

Tjeerd Thuss

to obtain the degree of Master of Science

at the Delft University of Technology,

to be defended publicly on Wednesday, August 27 at 3:00 PM.

Student number: 5104734

Project duration: November 18, 2024 – August 27, 2025

Thesis committee: Prof. Dr. ir. M. J. Tenpierik, Delft University of Technology
Dr. ir. H. R. Schipper, Delft University of Technology

Cover: Ultimaker S5 3D printing the final model of the thesis

An electronic version of this thesis is available at http://repository.tudelft.nl/.

TU Delft

Preface

Before you lies my master thesis about the optimization of a quarter-wavelength tube system for low frequencies, which is the last assignment of the Civil Engineering master at Delft University of Technology, with a specialisation in structural engineering. The thesis is a perfect representation of different skills I have learned during my studies in Delft: coding, modelling and data processing of real-life measurements. Besides, this thesis has broadened my horizons by introducing me to additive manufacturing.

Although sound isolation might not seem the most obvious subject for a structural engineering student, I was always very interested in this subject. After structural engineering, my interests were also very much towards architecture and especially building physics. This may be due to my greatest interest outside of my studies: music. Therefore, to do research with sound inside of my civil engineering program was the perfect combination of both worlds.

First of all, I would like to thank my supervisors Martin and Roel. Although I have received a small introduction to sound absorption during my regular master's program, I could not have finished my thesis without their help. I really appreciated the feeling that for some problems, me and my supervisors really both tried to fix the problem. For example, when both Martin and I tried separately to get the COMSOL model working, or when Roel and I both thought how to design the 3D printed model in the most efficient way. I felt really encouraged during my entire thesis and therefore I am very grateful to them.

I also want to thank my mom and dad. When I got home after a long day, they were also very interested in what I did and they really thought along with me when I encountered problems. They were looking forward to it as much as I was when I went to Delft to pick up yet another 3D printed ”creature”. To get the print airtight almost sometimes felt like a family team effort.

My gratitude also goes to my friends I made during my six years of studies in Delft. They really made it worth the effort to take the train each and every day back and forth to Delft. As most of them also still lived outside of Delft, they also ensured I would often get out of the ”Delft bubble”.

I look back on my time at Delft with great pleasure. Not only because of my academic development, but also due to other experiences. Highlight for me will be my trip to Japan and Thailand with the study association of Civil Engineering. Also smaller trips, day to day life at the faculty of CEG and other activities outside of the lecture desks really made my study time more enjoyable than I could have expected.

I hope you, the reader, will enjoy this thesis and it may inspire you to use the proposed soundproofing solution yourself.

Tjeerd Thuss
Delft, August 2025

Summary

This thesis presents the optimization of a quarter-wavelength tube (QWT) system for the absorption of low frequency sound in the range of 88 to 355 Hz. Low frequency noise, often generated by sources such as traffic, heavy machinery, and HVAC systems, present significant challenges in building acoustics due to the large material thickness required for absorption. This study proposes a compact, efficient, and customizable solution using quarter-wavelength tubes. These tubes can be connected with each other not only in series, but also in parallel. The configuration considered in this thesis is a combination of the two different combination types.

The goal of this research is twofold:

- To maximize the absorption of QWT systems in the aforementioned low frequency bandwidth.
- To minimize the volume of these QWT systems to improve the possibility of incorporating them into sound absorbing panels and to reduce the material use of the systems.

To achieve this, a methodology consisting of three different types of analysis is used.

- Analytical analysis: A Python code is designed for the optimization of the QWT system. This code consists of two parts: The part where the absorption coefficients of a QWT system is calculated using the recursive formulation, and the part where the dimensions and number of tubes of the system are optimized using the evolutionary algorithm DEAP. The most optimal system is used for the next analyses.
- Numerical analysis: Finite element analysis (FEA) was performed in COMSOL Multiphysics (in short: COMSOL), using both Pressure Acoustics physics with Narrow Region Acoustics and Thermoviscous Acoustics interfaces. These simulations provide more accurate absorption coefficient results than the analytical Python code, as three-dimensional thermoviscous effects are considered in more detail.
- Experimental analysis: Scaled prototypes were 3D printed using PLA and tested in an impedance tube to measure their real-world performance.

The final optimized QWT system using DEAP achieved broadband low frequency absorption while being significantly more compact than traditional absorbers. This system consists of one main tube connected in series to five parallel tubes. Optimization caused a decrease of 2731 cm^3 of air volume in the QWT system, while the absorption coefficient only slightly decreased. Less air volume in the system means that the different QWTs can be smaller, so less material is needed.

The analytical and numerical results aligned very well, but the experimental results were slightly off. This may be caused by the lack of complete airtightness of the model or the presence of undissolved support material (PVA).

From an engineering perspective, this research showcases how QWT systems can be optimized to effectively absorb low frequencies. Different boundaries can be entered into the optimization code, which makes it possible to design an optimized QWT system for every situation. This is especially useful where space or thickness is limited for traditional sound absorption.

In conclusion, this thesis bridges theoretical acoustics, computational modelling, and practical engineering, resulting in a tunable, space-saving soundproofing solution that can be adapted for real-life application. Further research may include the application of different materials or testing such systems on a large scale.

Contents

Nomenclature

Symbol	Description	Unit
a	Distance between QWTs in a panel	m
A_{eq}	Total equivalent sound absorption area	m^2
A_{tube}	Cross-sectional area of a tube	m^2
A_{wall}	Surface area of the wall containing tubes	m^2
c	Speed of sound	m/s
c_0	Speed of sound in air	m/s
C_p	Specific heat at constant pressure	J/(kg·K)
C_v	Specific heat at constant volume	J/(kg·K)
d	Diameter of a tube	m
d_{ec}	End correction length	m
f	Frequency	Hz
G	Viscothermal coefficient	–
H_{2p}	Transfer function (2-microphone method)	–
J_0, J_2	Bessel functions of first kind (orders 0 and 2)	–
k	Wave number	rad/m
k_r	Reduced frequency	–
L	Tube length	m
L_p	Sound pressure level	dB
l	Characteristic length of cross section	m
n	Polytropic coefficient	–
N	Number of tubes	–
p	Sound pressure	Pa
p_0	Reference sound pressure (20 µPa)	Pa
p_{eff}	Effective sound pressure	Pa
p_1, p_2	Pressure at microphones 1 and 2	Pa
R	Radius of a tube	m
R_2	Radius of main tube	m
R_i	Reflection coefficient (impedance)	–
$R_i(x)$	Reflection coefficient (impedance-based) at different positions	–
r	Reflection coefficient (energy-based)	–
s	Shear wave number	–
T	Reverberation time	s
$u(x)$	Particle velocity	m/s
V	Volume of room or tube configuration	m^3
x	Position in the tube	m
α	Absorption coefficient	–
$\bar{\alpha}$	Average absorption coefficient	–
γ	Ratio of specific heats (C_p/C_v)	–
δ_v	Viscous boundary layer thickness	m
δ_t	Thermal boundary layer thickness	m
η	Shear viscosity	Pa·s
λ	Wavelength	m
λ_{tc}	Thermal conductivity	W/(m·K)
μ	Dynamic viscosity	Pa·s
ρ_0	Density of air	kg/m^3
σ	Square root of Prandtl number	–
ζ	Acoustic impedance	Pa·s/m

ζ_{wall}	Wall impedance scaled with porosity	Pa·s/m
Ω	Porosity (open area ratio)	–
ω	Angular frequency	rad/s
Γ	Viscothermal wave number (complex)	–
Z	Acoustic impedance (pressure/velocity)	Pa·s/m
Z_0	Characteristic acoustic impedance ($\rho_0 c_0$)	Pa·s/m
Z_a	Specific acoustic impedance	Pa·s/m

1

Introduction

1.1. Research motivation

Sound proofing is one of the most dominant topics in acoustic research. A lot of focus is on sound consisting of low frequencies, as this kind of noise is an issue in many different environments. These types of noise are produced by sources such as heavy machinery, vehicles, and HVAC (heating, ventilation, and air conditioning) systems (Berglund et al., 1996). The biggest problem of low-frequency noise, often considered lower than about 250 Hertz, is that absorption of them requires thick materials. Long wavelengths, corresponding to low frequencies, are absorbed by materials that have a thickness at a quarter-wave distance, because the waves vibrate the most at these positions. Low frequencies could cause different types of annoyance, such as headaches, irritation, and unusual tiredness (Waye, 2011). Furthermore, such low-frequency noise can reduce productivity in workplaces and negatively impact the quality of life in urban areas. low-frequency noise can also cause structural vibrations. These problems need innovative solutions to be able to absorb these frequencies, but still limit material usage and spatial occupation. As a possible solution, quarter-wavelength tubes are developed. These tubes offer high absorption at very specific frequencies through acoustic resonance and viscothermal effects (Zwikker & Kosten, 1949). Combining tubes with different lengths and diameters and connecting them in series or parallel will offer a broadband absorption solution.

1.2. Problem statement

Although quarter-wavelength tubes, or QWTs, show great potential, there are still some significant research gaps. First of all, most extensive research focuses on higher frequencies. For instance, the research of Van der Eerden (2000) focuses mainly on frequencies higher than 1000 Hertz, and some configurations for lower frequencies are covered, but they are often just for the purpose of example and far from optimized. This is also the second problem which is still the case for QWTs: only some configurations of in-parallel and in-series connected tubes are researched. These configurations lack optimization, mainly in the area of combining in-parallel and in-series connected tubes. Finally, which also has to do with optimization, is that efficient material usage lacks further research: tubes for low frequencies are often big in size and therefore use a lot of space and material. In times where sustainability becomes more and more important, this will also apply for QWT-configurations.

1.3. Research objective

This research project aims to find the optimal combination of quarter-wavelength tubes connected in series with multiple parallel tubes to absorb frequencies between 88 and 355 Hertz. These frequencies are the lower bound of the octave band centered at 125 Hertz and the upper bound of the frequency centered at 250 Hertz. The optimization will be based on maximization of the absorption coefficient for these specific frequencies and minimization of the volume of the tube configuration. To do so, the effects of changing tube dimensions and different configuration types should be determined in detail.

In this research, only the previously mentioned frequencies between 88 and 355 hertz will be aimed to be absorbed. These two octave bands were chosen because they belong to the low-frequency sound spectrum. For the design of the configuration, only a primary main quarter-wavelength tube and smaller secondary connected tubes are considered: a third row of tubes connected in series is not considered. For optimization, only variation in tube diameter, variation in length, and number of parallel tubes will be considered. The diameter will be chosen in a way that planar acoustic waves can be considered. All tubes will be made of the same material, with the only requirement that the material must be airtight.

1.4. Research questions

The main research question of the thesis will be the following: What is the optimal configuration using minimal volume of a main quarter-wavelength tube connected in series with multiple parallel tubes for the absorption of frequencies between 88 and 355 Hz?

To answer this main question, the following sub-questions are proposed:

- How do changing the diameter, the length, and number of secondary quarter-wavelength tubes influence the absorption of the whole system?
- For which configurations does the system reach the maximum absorption?
- How do the numerically and analytically received absorption coefficients compare to the experimental results?

1.5. Reading guide

The structure of this thesis will be as follows: first, background information and the underlying theory will be explained for this topic. Then, the method of the research will be elaborated. This will be followed by the results of each simulation. Both the method as the results will consist of three parts: analytical, numerical, and experimental. The analytical part is used to propose an optimized quarter-wavelength tube system, the numerical part is used to do more precise simulations with the proposed system, and the experimental part is used to research how the system functions in real-life. Further elaboration will be given in the Methods chapter. The results will be followed by a chapter including a discussion based on the results, and finally the conclusion of the thesis will be presented, followed by a chapter including some further recommendations. The complete framework of the thesis is presented in Figure 1.1.

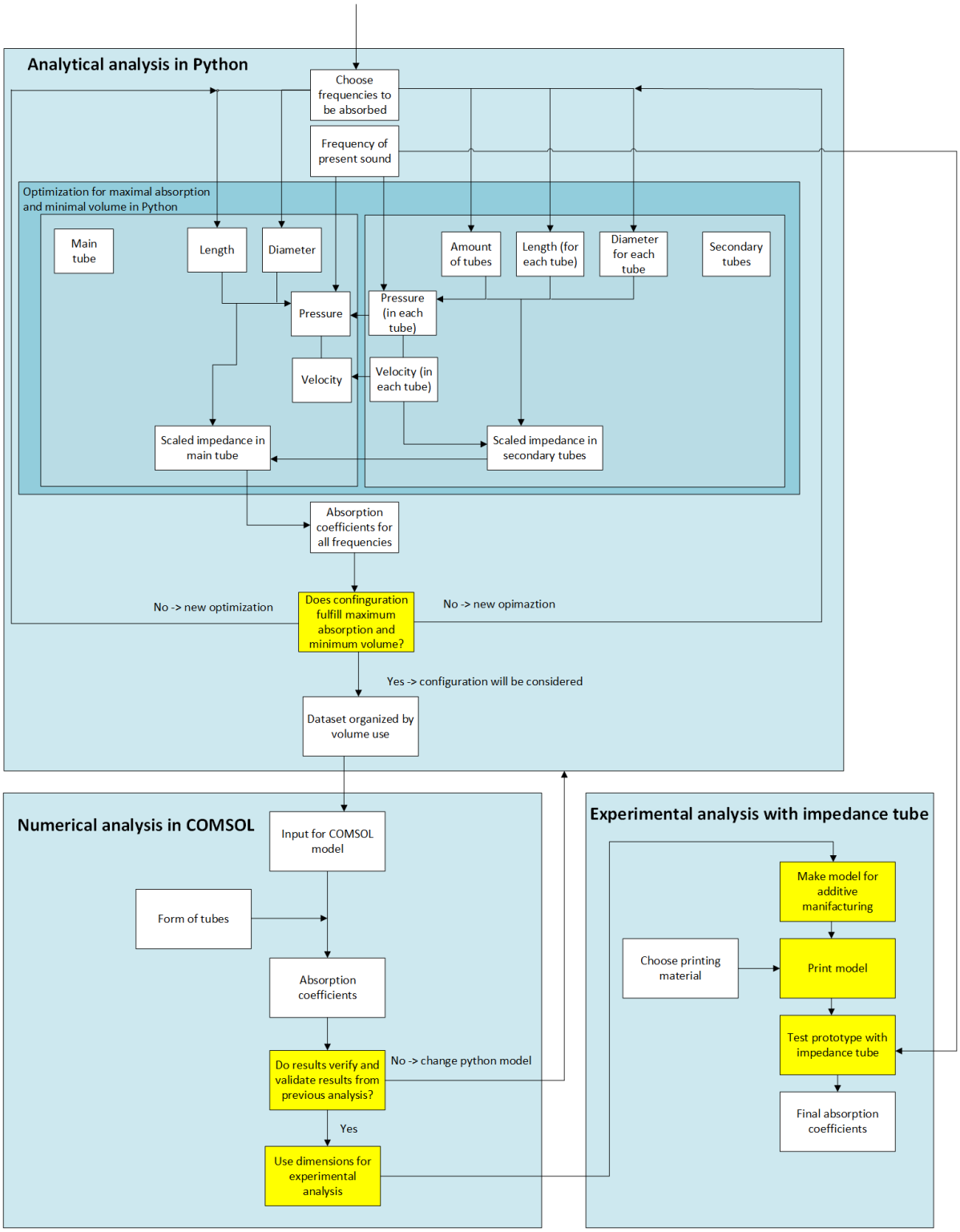

Figure 1.1: Framework of the thesis

2

Background

In this chapter, the background knowledge of quarter-wavelength tubes will be explained. This background knowledge is essential to understand the main principles, applications, and challenges of the quarter-wavelength tubes. With this knowledge the first sub-question can be answered:

- How do changing the diameter, the length, and number of secondary quarter-wavelength tubes influence the absorption of the whole system?

First, the essentials of sound absorption will be explained, consisting of the basic concepts of sound, sound absorption, and sound absorbers. Afterwards, the main theory and other essential characteristics of quarter-wavelength tubes will be explained.

2.1. Sound absorption essentials

Quarter-wavelength tubes are sound absorbers, so an understanding of sound absorption is essential to understand such tubes. However, in order to understand sound absorption, the basic working principles of sound should also be understood. Therefore, the basics of sound will be explained initially, followed by the theory of sound absorption. This will be followed up by some examples of existing sound absorbers with their advantages and disadvantages.

2.1.1. Basic concepts of sound

Characteristics of sound wave

Sound can be described as a variation in air pressure that propagates from a source through a medium that could be heard by the ear. It propagates as a longitudinal wave and varies in amplitude and frequency. The amplitude of a sound wave determines the volume of the sound, and the frequency determines its pitch. The amplitude is also responsible for the effective pressure of the sound, which will be explained more deliberately. The frequency is defined as the number of sound wave cycles occurring in one second, with the unit hertz (Hz). Humans are capable of hearing frequencies between 16 and 20,000 Hz. The human ear is most sensitive to frequencies between 1000 and 5000 Hz. If the sound consists of only one frequency, then it is a pure tone. Mostly, sound waves are composed of multiple individual waves, so most of the sound waves will not consist of one sine wave. The distance between two identical points of the wave is called the wavelength (λ).

Sound waves travel with a speed of sound that differs for different temperatures, It could be determined with $c_0 = (331.3 + 0.606 * T_C)$, where c_0 is the speed of sound in air in m/s and T_C the temperature in °C. The wavelength and frequency of sound waves are linked with each other by the speed of sound. The following formula describes the relationship between the different quantities:

$$\lambda = \frac{c}{f} \tag{2.1}$$

In this formula, c is the speed of sound in a random medium in m/s and f the frequency in hertz. A

conclusion that can be drawn immediately is that smaller frequencies come with bigger wavelengths. This conclusion is important as a foundation for this thesis.

Sound pressure level

As just described, sound waves are pressure waves. This means that when hearing sounds, the ear feels pressure. The human ear is very sensitive to pressure changes, but it does not hear fluctuations in pressure. The ear hears the energy contained by the pressure wave and it can be described with the following formula:

$$p_{eff} = \sqrt{(\frac{1}{t_2 - t_1} \cdot \int_{t_1}^{t_2} p^2 dt)} \tag{2.2}$$

In this formula, t_1 and t_2 are the boundaries of the time period when the sound is perceived in seconds, and p is the sound pressure in Pa. To measure the physical loudness of a sound wave, the sound pressure level formula (SPL, L_p) is used. This formula, expressed in decibels (dB), is logarithmic, as the human ear perception of sound loudness is also logarithmic. In addition, the hearing limits are between 20 μPa (threshold of hearing) and close to 200 Pa (pain threshold), which is a wide range. This range is covered by the logarithmic SPL, which only ranges between 0 and approximately 140 dB. This makes comparisons much easier, and additions of different sound sources are also easier to do with SPL. The SPL is the following formula:

$$L_p = 10 \cdot \log{(\frac{p_{eff}^2}{p_0^2})} \tag{2.3}$$

p_0 is the hearing threshold, so 20 μPa. However, this is the case in combination with a frequency of 1000 Hz, which also holds for the pain threshold. The human ear actually perceives sound differently for different frequencies. Higher and especially lower frequencies than 1000 Hz are perceived as less loud. This difference is greater for low SPLs than for higher SPLs. These differences can be presented with equal-loudness contours (see Figure 2.1

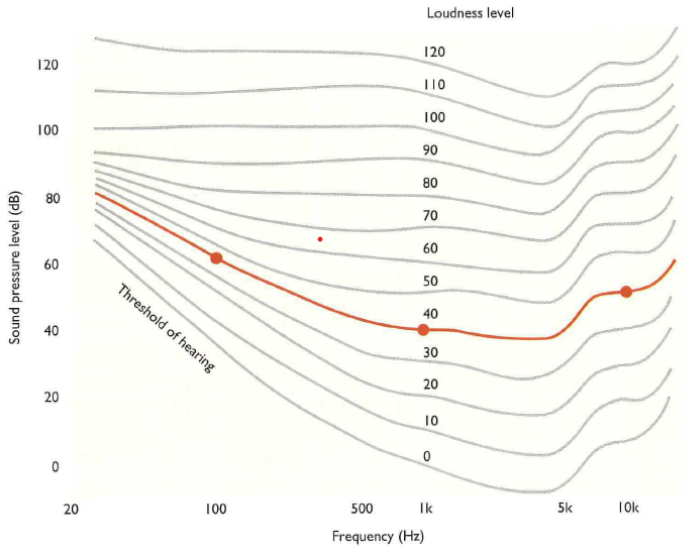

Figure 2.1: Equal-loudness contours for pure tones (Salter, 1998)

Absorption of sound decreases the SPL of sound waves. Understanding of the mechanisms behind SPL calculations is therefore essential.

Octave bands

Sound waves consist mostly of multiple frequencies, which makes them very complex. However, human ears still tend to integrate heard frequencies in different ranges. Therefore, sound wave analysis is often done with so-called *octave-bands* or *one-third-octave-bands* (Salter, 1998). The division in (one-third-) octave-bands could be compared with how a prism divides light into certain colour bands. The bands are used for sound measurements because they are able to present the content of sound of a sound source in a more understandable way than when just the whole sound wave is shown undivided.

Table 2.1 shows the frequency limits of the octave band division up to 1420 Hz.

Table 2.1: Octave-Band Frequencies

Lower Band Frequency [Hz]	Center Frequency [Hz]	Upper Band Frequency [Hz]
11	16	22
22	31.5	44
44	63	88
88	125	177
177	250	355
355	500	710
710	1000	1420

These bands will be used to determine for which frequency domain the absorption system will be optimized. As the main focus will be on the low-frequency sound spectrum, the bands with central frequencies 125 and 250 Hz are chosen. This means that the lower limit will be 88 Hz and the upper limit 355 Hz. In this way, a broad, still reachable, absorption band is achieved. 88 Hz is chosen as the lower limit, as a tube for the absorption of such frequency will have a length of approximately 1 meter. A tube of this length will not be too large to coil in an absorption system. More about such a system will be explained in 2.2.

2.1.2. Sound absorption

Reverberation time

In a closed room, sound is enclosed, and when the sound produced by a source reaches a boundary of the room, the sound will be reflected or absorbed by this boundary. Absorption of sound ensures that the sound will not be reflected in the room forever, so it decreases the SPL. The absorption and reflection are presented with coefficients (respectively α and r and added together they must be equal to 1.0 (so $\alpha = 1.0 - r$). It should be noted that r is the ratio of reflected *energy* over incoming *energy*. The time it takes for the SPL to decrease by 60 dB when the source is turned off is called reverberation time. The reverberation time is an important characteristic of a room to show its absorbent qualities. When the reverberation time is too long, almost all the sound is reflected, and the sound will blend. However, too short a reverberation time is also not optimal, as the sound will feel ”dead” and may be considered as unsettling by some people. When only high frequencies have very short reverberation times, the sound is conceived as hollow. If the room is highly absorbent for low frequencies, the sound is conceived as sharp. It is possible to have an estimate for the reverberation time by using the following formulas:

$$T \approx \frac{1}{6}\frac{V}{A_{eq}} \tag{2.4}$$

$$T \approx -\frac{1}{6}\frac{V}{S_{tot} ln(1-\overline{\alpha})} \tag{2.5}$$

Formulas 2.4 and 2.5 are respectively called Sabine’s and Eyring’s equations. In the formulas, T is the reverberation time in seconds, V is the volume of the room in cubic meters, A_{eq} is the total equivalent sound absorption area in square meters (more on this in the paragraph on the absorption coefficient),

S_{tot} is the total surface area of the room in square meters, and $\overline{\alpha}$ is the average absorption coefficient. These formulas will have approximately the same results for small absorption coefficients, but they will differ for larger coefficients.

Although no room measurements will be made during this thesis, an understanding of the effect of the absorption coefficient on other sound characteristics is of great importance.

Absorption coefficient

As mentioned above, sound will be absorbed or reflected when reaching a surface in a room. A small part of the sound will pass through the surface, but because this is such a small amount, it is often neglected. Absorption can happen in two forms: by friction in porous materials and by resonance. Absorption through friction will occur mainly for higher frequencies, and resonance is more effective for low and mid frequencies (Cox & D'Antonio, 2016). For both means, it holds that the vibrating energy of the sound wave is converted to heat.

Every material has its own absorption coefficient, so when determining the absorbent qualities of the entire room, A_{eq} is used. It can be calculated in the following way:

$$A_{eq} = \sum_{i=1}^{n} \alpha_i S_i \tag{2.6}$$

In formula 2.6, α_i is the absorption coefficient of the surface S_i. In Eyring's equation (formula 2.5, the average of these absorption coefficients is calculated ($\overline{\alpha}$) and multiplied with all surfaces summed together (S_{tot}).

Surfaces of a room are not limited to the boundaries of the room itself, such as walls and the ceiling, but also to, for instance, furniture and curtains. This means that it is difficult to determine the exact value of A_{eq}. For this thesis, only the absorption coefficient of the quarter-wavelength tubes system is needed because they are not placed in a room for measurements. However, it is important to understand that a small object with its corresponding absorption coefficient does not necessarily mean that the whole room will have this absorption for a certain frequency.

Acoustic impedance

Another important characteristic of sound and for the mechanism of making sound measurements is acoustic impedance. The acoustic impedance, Z, is the ratio of the perturbation of the pressure and of the velocity of a sound wave (Van der Eerden, 2000). Z is the resistance of a medium against vibration and oscillation and is most important for the reflection of the waves, as a sudden change in impedance will cause the sound wave to reflect. In addition, the acoustic impedance is strongly frequency-dependent.

When a plane wave travels freely, the impedance is called the 'characteristic specific impedance' (Z_o) and it can be calculated with $\rho_0 \cdot c_0$. ρ_0 is the density of air and c_0 is the aforementioned speed of sound in the air. It is characteristic for a medium, such as air in this instance. Specific means that planar waves are the case. The specific acoustic impedance (Z_a) is therefore the same as the original acoustic impedance, but per unit area.

Impedance is one of the main characteristics of absorption. A sudden change of impedance causes reflection of sound waves. The reflection coefficient R_i can be calculated with Formula 2.7 and is, unlike using incoming and reflected energy for r (see Section 2.1.2), calculated using impedances:

$$R_i(x) = \frac{Z(x) - Z_0}{Z(x) + Z_0} \tag{2.7}$$

When this reflection coefficient is known, the absorption coefficient can be determined with the following formula:

$$a = 1 - |R_i|^2 \tag{2.8}$$

In conclusion, impedance plays an important role in absorption and reflection, and therefore an understanding of this concept is vital.

2.1.3. Sound absorbers

There exist two main principles for sound absorbers, namely porous and resonant absorbers (Qiu, 2016). Porous absorbers are based on viscothermal effects, which cause the acoustic energy to dissipate. Resonant absorbers are based on, as the name implies, resonance effects. A more elaborate explanation of the viscothermal and resonance effects will be given in 2.2.1. Some important kinds of sound absorbers with their advantages and disadvantages will be presented which are based on these main principles.

Porous absorbers

The main principle of porous absorbers is that sound energy is lost due to the effects of the viscous boundary layer on the small interconnected pores of the porous absorber (Kuczmarski & Johnston, 2011). In other words, friction of the air in motion with the pore walls causes the wave to lose energy. However, the pores should not be too large or too small. When the pores are too large, no viscous effects will occur and the incoming sound wave will not be absorbed. When the pores are too small, it is not possible for a wave to penetrate sufficiently far in the absorber to cause absorption (see Figure 2.2.

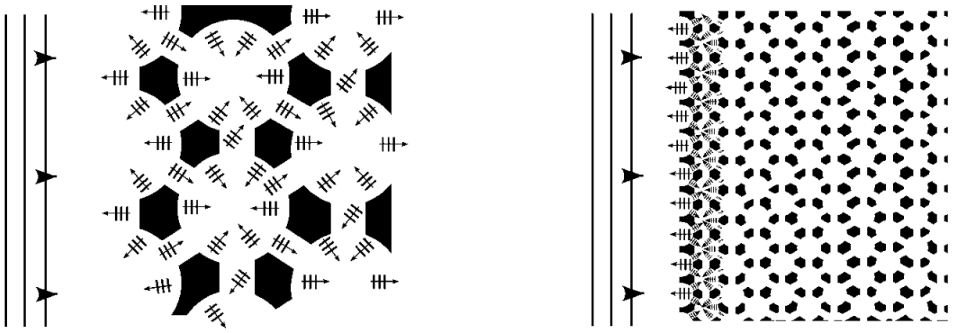

Figure 2.2: Decrease in energy transfer potential as pore size decreases from large (left) to small (right) (Kuczmarski & Johnston, 2011)

Porous absorbers that occur often are, for example, glass wool, foamed materials, and rock wool. The frequencies that a porous absorber can absorb are dependent on the thickness of such absorber. The thicker the porous absorber, the more frequencies it can absorb (in the lower direction). This immediately shows the advantages and disadvantages of porous absorbers: the advantage is that all frequencies can be absorbed if the material is thick enough, but the coherent disadvantage is that an absorber should be very thick to absorb low frequencies.

Panel absorbers

Panel absorbers, or membrane absorbers, consist of a lightweight plate in front of a volume, partially or completely filled with porous material (Ford & McCormick, 1969). The panel absorber acts as a mass-spring system, in which the front plate is the mass and the enclosed air in the volume the spring. The frequency that will be absorbed by the system is dependent on the tuning of the thickness of the air cavity and plate. For a certain frequency, the system will resonate. The resonance causes viscous effects that dissipate energy put into the system by the sound wave. This effect can be improved by adding porous material in the air cavity. An example of some kind of panel absorber can be seen in Figure 2.3.

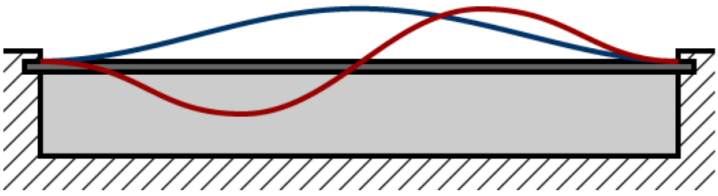

Figure 2.3: An inclined panel absorber in resonance (Hunecke, 2024)

The advantages of panel absorbers are that they are simple absorbers that are effective for low frequencies. However, the disadvantages are that they can only be tuned for a narrow band of frequencies, and panel absorbers are not effective for high frequencies.

Helmholtz resonator

A Helmholtz resonator is, as the panel absorber, based on a mass-spring system (Gommer, 2016). In this case, the volume inside the Helmholtz resonator is the spring, and the air inside the tube of the resonator is the mass (see Figure 2.4).

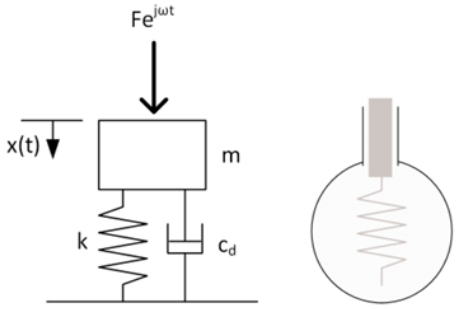

Figure 2.4: Working mechanism of a Helmholtz resonator, with k the spring stiffness, m the mass, c_d the linear viscous damping coefficient, $Fe^{j\omega t}$ the harmonious applied force and $x(t)$ the excitation of the mass over time (Gommer, 2016)

The solution of the differential equation defining the mass-spring system gives the frequencies for which the system will resonate. The absorption will mainly occur at positions in the resonator where the velocity is highest or where turbulent flow is the case, because most of the motion energy is transferred to internal energy. The advantages of Helmholtz resonators are that they have a very high narrow absorption peak for specific frequencies and that they are highly tuneable. However, the bandwidth of the absorption peak is even narrower than that of a panel absorber.

2.1.4. (Micro)-Perforated panel absorbers

Micro-perforated and perforated panel absorbers are absorbers that may sound the same but have different absorption principles. Micro-perforated panel absorbers are based on viscothermal damping, while perforated panel absorbers function through resonance. Perforated panel absorbers are actually a combination of a lot of Helmholtz absorbers: When a sound wave reaches a panel, the air in the holes oscillates back and forth, whereas the air behind the holes acts like a spring. Just as for Helmholtz resonators, the absorption will occur at the spot where the velocity is at its highest, and this motion energy will be transferred to internal energy. It is also possible to place porous material behind the perforated panel absorber. The advantages of perforated panel absorbers are that such panels are highly tuneable for low- and mid-frequency absorption, are more durable than porous materials, and are more aesthetically pleasing than other sorts of absorbers. Disadvantages include the need for careful design and placement, a narrow bandwidth without porous backing, and potentially higher manufacturing costs than those of other types of absorbers.

In addition, the resistance of the perforated panel absorbers must match the characteristic air acoustic resistance to receive high absorption, but wide absorption is only possible with a low mass (Maa, 1975).

This contraction is solved using micro-perforated panel absorbers. The holes of micro-perforated panels are between 0.05 and 0.1 mm, and due to this small size, a viscous boundary layer occurs, just like for porous absorbers. An example of a micro-perforated panel is given in Figure 2.5.

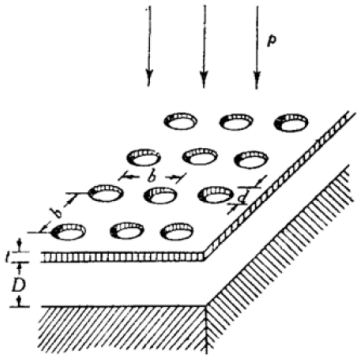

Figure 2.5: An example of a micro-perforated panel absorber (Maa, 1975)

Advantages and disadvantages of micro-perforated panel absorbers are mostly the same as for perforated panel absorbers, although micro-perforated panel absorbers do often not need porous backing, but they are even more expensive too.

2.2. Quarter-wavelength tubes

In this section, the main principles of quarter-wavelength tubes are described. First, the main theory of such tubes will be explained, followed by descriptions of the effects of their length and diameter and of connecting them in series or in parallel. Finally, the effect of the porosity of the tubes in a absorbing wall and the effect of bending the tubes will also be explained. Different geometries of the tubes, such as square or triangular, will not be considered.

2.2.1. Main theory

The quarter-wavelength tube (also known as QWT) is a tube that is used to absorb the sound of specific frequencies (see Figure 2.6). The QWT is closed at one end and open at the other. The theory of the functioning of these QWTs is that in the tube standing waves should occur, leading to resonance. This resonance is one of the two manners the QWT absorbs sound, next to viscothermal absorption. These two principles will now be explained in more detail.

Resonance

When the air in QWT resonates, a standing wave forms inside the tube. The standing wave has a pressure anti-node (maximal pressure) at the closed end and a node (zero pressure) at the opening. The anti-node and node will be opposite for air displacement. The resonance occurs because the sound wave reflects off the closed end and interferes constructively with the incoming waves. Specifically, when a compression wave reflects at the closed end, it travels back towards the opening and precisely meets the front of an incoming rarefaction wave (Field & Fricke, 1998). The rarefaction wave, together with the compression wave, forms one acoustic wave (and also one wavelength). To achieve that the reflected front of the compression wave will interact with the front of the rarefaction wave, the QWT should have half the length of a compression wave, so a quarter the length of a wavelength. The QWT will also function for any odd multiple of the quarter of the wavelength, so a QWT with a length of $3/4$ or $5/4\,\lambda$ will work for the same frequency.

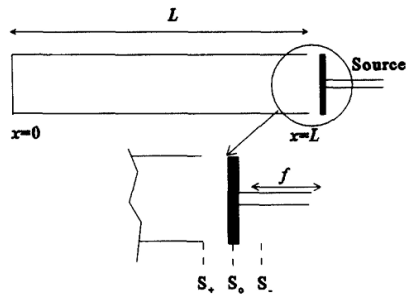

Figure 2.6: Typical quarter-wave resonator with a source of continuous vibration (Field & Fricke, 1998)

The standing wave occasion does not directly explain the absorption qualities of the QWT. However, because a pressure node is always present in the opening, destructive interference will occur at this spot. The pressure will then have the same value as the atmospheric pressure value. For air particles, the opposite will happen: an anti-node at the opening and a node at the closed end. Therefore, air is still able to leave (and enter) the tube. The destructive interference of the acoustic wave does not influence the standing wave in the QWT. The particles are able to move, so an increase of pressure (at the closed end, the pressure is twice the amplitude of the incoming wave) is still possible. The standing wave in the tube will proceed as long as the wave (with the same frequency) enters.

The sound wave in a prismatic tube can be predicted with the reduced one-dimensional Helmholtz equation (Van der Eerden, 2000). This function (2.9) excludes the time dependency, which can only be done in the specific case of a harmonic wave. To receive the time-dependent response of the wave, the reduced Helmholtz equation should be multiplied by $e^{i\omega t}$. The equation itself reads:

$$p(x) = \hat{p}_A \cdot e^{kx} + \hat{p}_B \cdot e^{kx} \tag{2.9}$$

$\hat{p}_A$ and $\hat{p}_B$ represent the amplitude of the pressure in the direction of the opening of a tube and the amplitude of the pressure in the direction of the closed end, respectively. These amplitudes can be determined by considering the boundary conditions of the tube, which will be a pressure, velocity, and/or impedance condition. k is the wave number and is calculated with $2\pi/\lambda$. x is the displacement in the tube, with the The particle velocity can also be obtained using the reduced Helmholtz equation and the linearised momentum equation:

$$u(x) = \frac{-1}{Z_0} \cdot (\hat{p}_A \cdot e^{kx} - \hat{p}_B \cdot e^{kx}) \tag{2.10}$$

Viscothermal effects

Resonance in a QWT is not the main factor for absorption of sound waves. Viscothermal effects, because of the narrow size of the tube, are mainly responsible for the absorption. The viscous and thermal effects have a huge influence on the propagation of a wave (Beltman, 1999). Both phenomena cause a boundary layer near the walls of the tube, where a loss of energy occurs as a result of viscous shear stress and thermal energy dissipation. The loss of energy causes a decrease in the amplitude of the sound wave. These viscothermal effects are included in the reduced Helmholtz equation with the so-called *low-reduced frequency model*. This model was developed by Zwikker and Kosten (1949) and proven by Tijdeman (1975). Beltman changed the model to a dimensionless form. Equations 2.9 and 2.10 are adjusted to the following equations:

$$p(x) = \hat{p}_A \cdot e^{\Gamma kx} + \hat{p}_B \cdot e^{-\Gamma kx}, \tag{2.11}$$

$$u(x) = \frac{G}{Z_0} \cdot \left(\hat{p}_A \cdot e^{\Gamma kx} - \hat{p}_B \cdot e^{-\Gamma kx}\right) \tag{2.12}$$

The main difference between the equations is the viscothermal wave propagation coefficient (Γ) and the coefficient G, which contains the influence of a different cross section. The complex quantity Γ covers the viscothermal character of the sound wave in the QWT, where the real part accounts for the

attenuation of the wave and $\frac{c_0}{\mathrm{Im}(\Gamma)}$ for the phase velocity. Γ and G can be calculated with the following two formulas:

$$\Gamma = \sqrt{\frac{J_0(i\sqrt{i}s)\,\gamma}{J_2(i\sqrt{i}s)\,n}} \tag{2.13}$$

$$G = -\frac{i}{\Gamma}\frac{\gamma}{n} \tag{2.14}$$

J_0 and J_2 are Bessel functions of the first kind of order 0 and 2. n is a polytropic coefficient and is calculated with this formula:

$$n = \left(1 + \frac{\gamma - 1}{\gamma}\frac{J_2(i\sqrt{i}s\sigma)}{J_0(i\sqrt{i}s\sigma)}\right)^{-1} \tag{2.15}$$

$$\tag{2.16}$$

s is the shear wave number, k_r the reduced frequency, σ the square root of the Prandtl number and γ the ratio of the specific heats. All four parameters are dimensionless and are characteristic of the low-reduced frequency model. They can be determined with the following four formulas:

$$s = l\sqrt{\frac{\rho_0\omega}{\mu}} \tag{2.17}$$

$$k_r = l\frac{\omega}{c_0} \tag{2.18}$$

$$\sigma = \sqrt{\frac{\mu C_p}{\lambda_{tc}}} \tag{2.19}$$

$$\gamma = \frac{C_p}{C_V} \tag{2.20}$$

In these four formulas, l is the characteristic length of the cross-section (the radius in case of a tube) in meters, ω the angular velocity of the wave in radials per second, μ the dynamic viscosity of the medium in pascals times seconds (18.2 10^{-6} for air at 20 °C), C_p is the specific heat at constant pressure in joule per kelvin per kilogram, C_V the specific heat at constant volume in joule per kelvin per kilogram and λ_{tc} the thermal conductivity in Watts per meter kelvin. σ and γ are constant for an ideal gas and are approximately 0.84 and 1.4 respectively. s and k_r are important parameters for the low-reduced frequency model, as they indicate if viscothermal effects are occurring in a tube.

2.2.2. Effect of length and diameter

Length of a tube

The length is the most important geometric parameter of the QWT. As explained in 2.2.1. The tube has to have a length that is a quarter of the wavelength of the corresponding frequency. However, a QWT is also sensitive to inlet effects, which causes the effective length of a QWT to be slightly longer (Rayleigh, 1945). This end correction will be determined with the following formula:

$$d_{ec} = \frac{8R}{3\pi} \tag{2.21}$$

The end correction causes a small shift of the absorbed frequency (see Figure 2.7). However, the amount of absorption is not affected. R is the radius of the tube and Ω is the porosity of a panel, which will be explained further in 2.2.6. a is the distance between two QWTs in a panel.

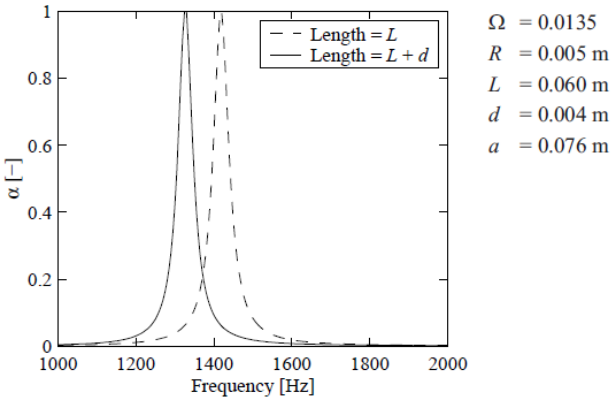

Figure 2.7: Inlet effects for a wall with resonators. (Van der Eerden, 2000)

Not only do tubes directly connected to the outer side of an absorption panel experience inlet effects, parallel connected tubes experience a small form of inlet effects as well. Formula 2.22 will have a small adjustment for this case:

$$d_{ec} = \frac{8R}{3\pi}(1 - 1.25\frac{R}{R_2}) \tag{2.22}$$

R_2 is the radius of the main tube in meters and R of the parallel connected tube.

Diameter of a tube

The diameter of the tube has a small influence on the place of an absorption peak, but mainly on the viscous and inertial effects (Costa, 2016). A smaller radius causes broader absorption than a larger radius. These effects can be seen in the graph in Figure 2.8.

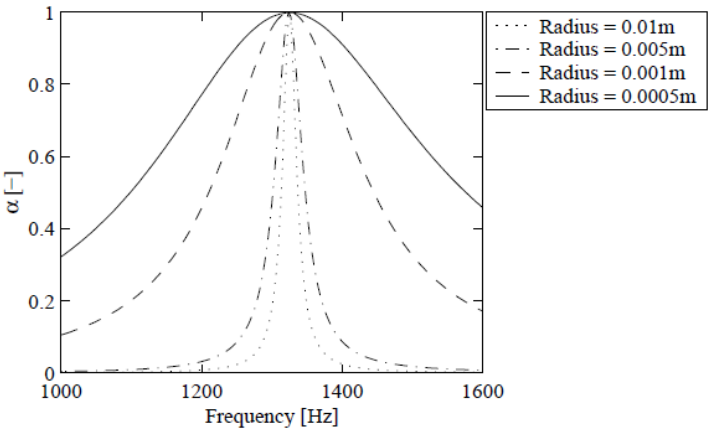

Figure 2.8: Effect of different radii for a quarter-wave resonator tuned at 1324 Hz (Van der Eerden, 2000)

The wider absorption peak is mainly caused by viscous losses in the tube. The viscous losses have an effect on the porosity in addition to the effect of smaller diameters, but this will be explained in more detail in Subsection 2.2.6. When the radius becomes very small, the tubes even mimic the absorbing effects of certain foams, such as glass wool.

In addition, the diameter also has a small effect on the end-correction of length of the tube, so actually also on the absorbed frequencies.

2.2.3. In-series connected tubes

In a wall consisting of a QWT system, the tubes can be connected in two ways: in series and in parallel (and combinations of them). When a QWT is connected to another QWT in series, it means that the

second QWT is connected axially at the end of the first QWT (see Figure 2.9. This means that the end plate of the first tube will have an opening for the second tube. As plane waves are considered in the system, the tube connected in series does not have to be centrally connected to the first tube. It is possible that the second tube has a bigger diameter than the first tube, but for this thesis the focus will only be on connected tubes with a smaller diameter than the main tube.

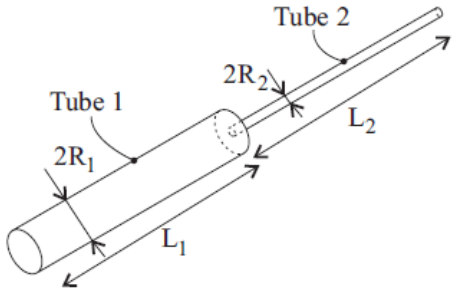

Figure 2.9: Two axially coupled tubes (Van der Eerden, 2000)

For tubes connected in series, the impedance characteristic is dominated by the first tube for most frequencies (Scholten, 2018). The first tube will act as an open tube for the resonance frequencies of the in-series connected tubes. This means that the first tube will have a pressure release at its end instead of a rigid wall. The pressure release slightly changes the absorption of the first tube as the resonance frequency slightly shifts to the left.

The results of a typical QWT system connected in series compared to the main tube without a connected tube can be seen in Figure 2.10. It can be seen in the figure that the main tube has an effect on the central frequency of the absorption width. By tuning the lengths and diameters of the tubes correctly, a high-absorption spectrum for a relatively broader frequency band can be obtained.

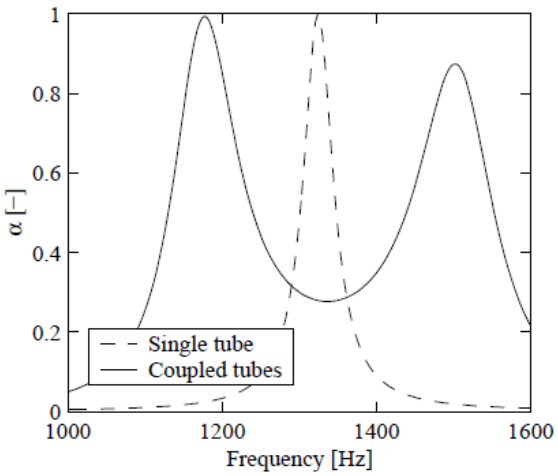

Figure 2.10: Two axially coupled tubes in comparison to a single tube (Van der Eerden, 2000)

2.2.4. In-parallel connected tubes

In-parallel connected tubes mean that the tubes are placed next to each other (see Figure 2.11). The result of this type of configuration may not be surprising, as the absorption spectrum will have peaks for the corresponding different tube lengths. However, this may not be completely true, as the porosity of the tubes also has an effect on the absorption of the tubes, but this will be explained in Section 2.2.6.

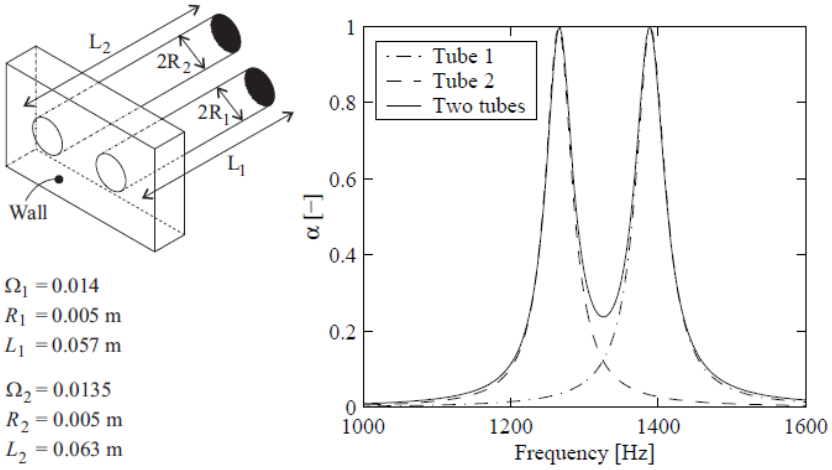

Figure 2.11: Two parallel connected tubes with their absorption spectrum. Ω_1 and Ω_2 are the porosities of the tubes (Van der Eerden, 2000)

2.2.5. Combination of in-series and in-parallel connected tubes

It is also possible to combine the two options of QWT configurations. This is done by placing the tubes in parallel after the first tube, so that each parallel tube is connected in series to the first tube (see Figure 2.12). An advantage of such configuration is that this results in a more optimal use of space than just placing multiple tubes in series after each other or a lot of tubes next to each other. This configuration offers promising results, as the absorption width is wider than that of a series connected tube and parallel connected tubes.

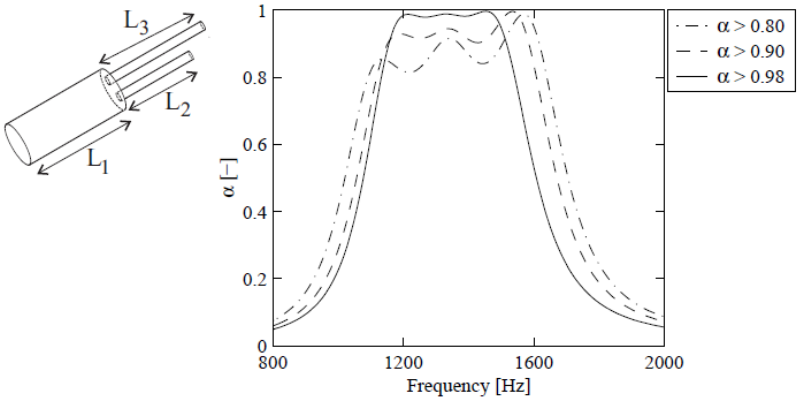

Figure 2.12: Multiple connected tubes for different lengths and widths. See the research of Van der Eerden (2000) for full details

2.2.6. Porosity

If a certain QWT system is placed many times in a wall, the wall will show different absorption spectra for different amounts of QWTs per area. This effect is due to the porosity of the wall (Van der Eerden, 2000). Porosity is defined with the following formula:

$$\Omega = \frac{NA_{tube}}{A_{wall}} \tag{2.23}$$

In this formula, N is the number of identical QWTs, A_{tube} the cross-sectional area of a single QWT, and A_{wall} the total wall area. When the porosity is known, the absorption of the whole wall, including QWTs, can be determined by initially calculating the ”scaled” impedance of the wall.

$$\zeta_{wall} = \frac{\zeta_{tube}}{\Omega} \tag{2.24}$$

Or for a wall with multiple kinds of QWTs:

$$\zeta_{wall} = \frac{1}{\sum \frac{\Omega_j}{\zeta_j}} \tag{2.25}$$

In these formulas, ζ_{tube} (or ζ_j) is the scaled impedance for one kind of QWT. The scaled impedance is calculated with Formula 2.26:

$$\zeta(x) = \frac{-G}{Z_0} Z_a(x) \tag{2.26}$$

The reflection could also be calculated using this scaled impedance, using $R(x) = \frac{\zeta(x) - 1}{\zeta(x) + 1}$. This formula shows that maximum absorption is received for $\zeta = 1$. The main conclusion of this relationship is that if the impedance of a tube is matched with the corresponding porosity in such a way that $\zeta_{wall} = 1$, the maximum absorption for the combined QWT system is obtained. This is an important design conclusion when QWTs are included in an absorption wall.

2.2.7. Coiling of tubes

Although QWTs already decrease the volume necessary for sound absorption, the length can still be quite long for low frequencies. For example, 88 Hz requires a QWT with a length of around 0.97 metres. To limit such thicknesses, it is also possible to coil the QWTs (Cai et al., 2014). An example of a bent tube is shown in Figure 2.13. Bending a QWT results in almost the same results as leaving the QWT straight, except for a small acceptable shift of the resonance frequency and a small gain of the absorption coefficient (Cambonie et al., 2018).

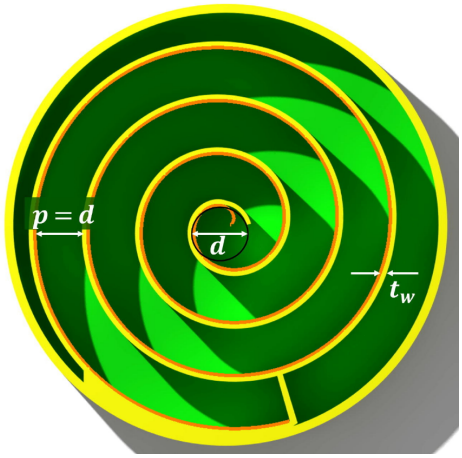

Figure 2.13: Front section of a spiral resonator with d the diameter, t_w the thickness of the tube wall and p the distance between two central lines (Catapane, Petrone et al., 2023)

In the ideal scenario, the bending pattern will only be two-dimensional. However, if the area of the wall is limited on its sides, the QWT should also show a 3-dimensional pattern. This will, for instance, be needed when testing QWT samples in an impedance tube (see Section 3.3.3).

3

Methods

In this section, the methods will be described how to achieve a QWT system that will absorb as much as possible sound for the frequencies between 88 and 355 Hz, but still uses as little material (or volume) as possible. To achieve this, the system will be analysed in three different ways: analytical, numerical, and experimental. Each analysis is a more detailed step to make a theoretically designed system physically possible. In addition, each method will be validated using existing results. First, the analytical analysis will be elaborated, followed by the numerical analysis and the experimental analysis.

3.1. Analytical analysis

The main goal of the analytical analysis is to obtain the ”best” solutions for the optimization problem, which consists in minimizing the use of the QWT system in total volume and maximizing the absorption of this system. To do so, the Python programming language will be used. The code will consist of two parts: the QWTs calculation part itself, where the absorption coefficients of the QWT system are received for the whole frequency bandwidth, and the optimization part, where the optimal solutions for the optimization problem are received. For calculations of the QWT system, the *recursive formulation*, which is presented by Bergh and Tijdeman (1965), will be used. For the optimization part, the Python package *DEAP* will be used.

3.1.1. Recursive formulation

The recursive formulation is based on a mass balance for a volume to which a number of tubes are attached (see Figure 3.1).

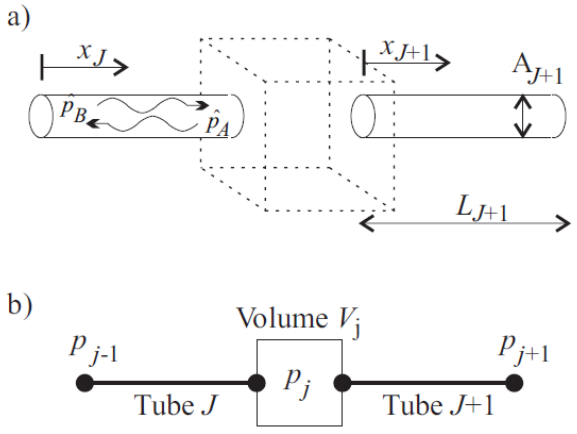

Figure 3.1: A geometric (a) and schematic (b) view of a volume with two tubes connected to it (Van der Eerden, 2000)

The method is based on the assumption that the mass variation due to a change in the density of the volume V_j must be equal to the difference between the mass leaving the volume and the mass entering the volume. In addition, boundary conditions, such as pressure or impedance conditions, should be known at the end of the tubes (or "branches"). The final result of the theory of the recursive formulation is the following formula:

$$\frac{p_j}{p_{j-1}} = \left[\cosh(\Gamma kL)_J + \frac{\sinh(\Gamma kL)_J}{A_J G_J}\left(-\frac{ik\gamma}{\eta_\nu}V_j + \frac{A_{J+1}G_{J+1}}{\sinh(\Gamma kL)_{J+1}}\left\{\cosh(\Gamma kL)_{J+1}\frac{p_{j+1}}{p_j}\right\}\right)\right]^{-1} \tag{3.1}$$

$\frac{p_j}{p_{j-1}}$ is the transfer function. It is a way to relate the pressure at the end of a tube to the pressure at the beginning. All other variables are explained in Section 2.2.1. In formula 3.1 the part that is multiplied by $\frac{A_{J+1}G_{J+1}}{\sinh(\Gamma kL)_{J+1}}$ is the part that covers a connected tube in series. To include more tubes connected in series with the same tube, the same part in the brackets should be repeated for each extra tube.

For a tube that is closed at one end, the boundary condition will be the following:

$$\frac{p_j}{p_{j-1}} = [\cosh(\Gamma kL)_J]^{-1} \tag{3.2}$$

Combining formula 3.2 with formula 3.1 and considering multiple tubes connected in series with the same volume and without the present volume, the following formula results:

$$\begin{aligned}\frac{p_j}{p_{j-1}} = &\left[\cosh(\Gamma kL)_J + \frac{\sinh(\Gamma kL)_J}{A_J G_J}\left(\sum_{n=1}^{N}\frac{A_{J+1,n}G_{J+1,n}}{\sinh(\Gamma kL)_{J+1,n}}\right.\right.\\ &\left.\left.\left\{\cosh(\Gamma kL)_{J+1,n} - [\cosh(\Gamma kL)_{J+1,n}]^{-1}\right\}\right)\right]^{-1}\end{aligned} \tag{3.3}$$

In the formulation of $J+1,n$, 1 represents the first row of tubes after the main tube and n is a specific tube connected to the tubes in the first row. Only tubes in the first row are considered and as these are multiple tubes, the formulation will be $J+1,n$. As described by Van der Eerden (2000), the impedance at the beginning of the QWT system can be determined with the following formula:

$$\zeta(0) = \frac{\sinh(\Gamma kL)}{\cosh(\Gamma kL) - \frac{p_1}{p_0}} \tag{3.4}$$

As $\frac{p_1}{p_0}$ is known thanks to the formula 3.3, the impedance, and therefore also the absorption coefficient (see Section 2.1.2), of the whole system can be calculated. This code is validated by comparing results for the same tube configuration as, for example, multiple tubes mentioned by Van der Eerden (2000). The full code is included in Appendix A.

3.1.2. DEAP

For the optimization part of the analytical analysis, the DEAP library in Python is used. DEAP (Distributed Evolutionary Algorithms in Python) is a framework for multi-objective optimization using evolutionary algorithms. For this study, the NSGA-II algorithm is used. NSGA-II (Non-dominated Sorting Genetic Algorithm II) is a form of multi-objective evolutionary algorithm, or MOEA (Deb et al., 2002). In contrast to other MOEAs, NSGA-II has a faster computation time and a mechanism that passes the best individuals directly to the next generation without cross-over or mutation (elitism approach).

Genetic algorithms are a class of optimization techniques inspired by the principles of natural evolution. They simulate the process of natural selection by generating a population of candidate solutions to a

problem, each represented by a set of parameters (or 'genes'). These individuals are evaluated using a fitness function that determines how well they perform with respect to the defined objectives. Over successive generations, the algorithm applies genetic operators such as selection (choosing the best individuals), crossover (recombining genes of two parents), and mutation (randomly altering genes) to create new individuals. This process allows the population to gradually evolve toward optimal or near-optimal solutions, even in complex and multidimensional problem spaces. Since genetic algorithms are stochastic in nature, results may vary slightly between runs. To account for this variability, the algorithm can be executed multiple times, and either the best or average Pareto front can be considered.

DEAP works by representing potential solutions as individuals in a population. Each individual consists of variables (for this study, the variables are tube lengths and diameters) and evolves over generations using evolutionary characteristics such as the before mentioned selection, crossover, and mutation. The evolution is guided by a fitness function that evaluates the performance of the individuals based on the objectives, which are minimizing the volume and maximizing the absorption over the octave bands. To ensure a more balanced optimization, the objectives are normalized before comparison at a later stage of the development of the code. This prevents the algorithm from favouring one objective over the other due to differences in numerical scale. The results before scaling are included in the final results section (see Section 4.1.1).

In the optimization, two variables will have boundary values to limit the outcomes:

- Tube lengths: the tubes will have lengths constrained between **0.01 m** and **1.0 m**
- Tube diameters: the diameters of the tubes will be constrained between **0.0001 m** and **0.1 m**

Additionally, a constraint is applied to ensure that the total cross-sectional area of the connected tubes does not exceed the cross-sectional area of the main tube. This reflects a realistic physical limitation for proper acoustic performance and manufacturability.

The two objectives are defined as minimizing total volume usage and maximizing absorption across the entire octave bandwidths. However, minimizing total volume usage is easily defined as receiving as small as possible lengths and diameters, the maximal absorption coefficient is harder to define. For maximization, two different types of distinguishing characteristics are defined:

- Maximum absorption: When maximum absorption is considered, it could be possible that only one sharp peak for a certain frequency will have maximum absorption, but the absorption of other frequencies will be minimal. As the goal is to maximize the absorption over the whole frequency band, two ways of maximizing are considered, namely receiving an as big as possible Area Under the absorption Curve (AUC), or receiving the highest average absorption values over the bandwidths.
- Bandwidth: To receive as great as possible absorption over the whole bandwidth, the bandwidth of 88 to 355 Hz is treated in three different ways with the goal of spreading the absorption peaks even more. The optimization is done with three different types of bandwidth: an optimization over the whole bandwidth, an optimization per octave band, or an optimization over third-octave bands (so an octave bands divided in three parts).

The goal of these methods of distinction is to evenly distribute absorption across the bandwidth while still maximizing the total absorption. When this is not done, the results will obviously contain a higher absorption at higher frequencies. This will be the case, as the volume is minimized and absorption of higher frequencies uses less volume (due to shorter lengths).

The DEAP-method uses, as mentioned before, some kind of evolutionary characteristics. The values of the characteristics can be chosen and have a great influence on the results. The four characteristics are the following.

- mu (μ): the number of individuals retained after selection.
- lambda (λ): the number of offspring generated per generation. It is often equal to or twice the value of mu
- cxpb: the crossover probability, so how characteristics of parents are exchanged to the offspring

- mutpb: mutation probability, so the probability of how some offspring are mutated for additional diversity.

mu is chosen as 150, lambda as 150, cxpb as 0.9 and mutpb as 0.1. These numbers are chosen to have a converging result without a computing time that will take a long time. The number of generations is set as 200.

The final results will be on the so-called ”Pareto front”. The Pareto front represents a set of non-dominated solutions, where no objective can be improved without sacrificing at least one other objective. For this study, each point on the Pareto front represents a trade-off between minimal volume usage and maximal acoustic absorption. For now, the five best solutions are withdrawn for each distinction from the results. The full code is included in Appendix B.

3.1.3. Verification and validation of analytical method

For further research of this thesis, it is of huge importance that the Python code actually gives the correct results. Therefore, the code should be verified and validated. Verification means that the Python code does not contain any errors and the used method is applied correctly. With validation, the code is compared to some trusted results to check if the code gives the correct results.

However, for the DEAP part of the Python code, it is harder to validate it, as DEAP is not applied to other QWT problems. Therefore, the Pareto front and the convergence graph are included for the final result (see Section 4.1.2).

verification of analytical method

For the verification of the analytical method, a simple QWT system is used to test the code. The QWT system will consist of just one tube, so the resonance frequency can be calculated by hand. For verification, a tube with a resonance frequency of 1000 Hz is used. The length of such a tube will be $\frac{343}{4 \cdot 1000} = 0.086\ m$. To also test the effect of the diameter, three different diameters will be used to show the shift in frequencies due to the end-correction phenomenon: 0.005, 0.01, and 0.05 m. Using 2.21, the new tube lengths are 0.088, 0.090, and 0.107 m respectively, which results in resonance frequencies of 975.9, 952.8,and 801.8 Hz. In addition, this means that the tube should have a shorter length if an exact resonance frequency of 1000 Hz is desired. The porosity is set at a fixed value of 0.03. The results of the Python code using the recursive formulation are given in Figure 3.2.

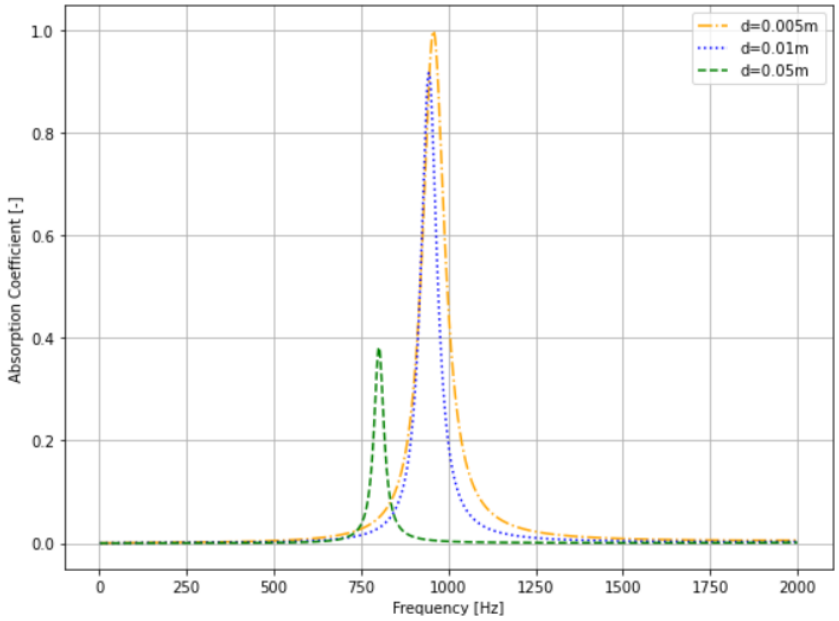

Figure 3.2: Absorption coefficients of three different quarter wavelength tubes with $L = 0.086\ m$ and $\Omega = 0.03$ using own Python code

Although the three peaks do not align exactly with the calculated values (from right to left: 957, 943 and 801 Hz), the results still verify the code. The main reason is that the porosity was not taken into consideration, and this has a considerable effect on the resonance frequency (and its corresponding absorption peak). As the ideal porosity is different for each diameter (see Section 2.2.6), the shifts of the resonance frequencies are different.

Validation of analytical method

To validate the code consisting of the recursive formulation, the results of Van der Eerden (2000) are used. Van der Eerden has used the recursive formulation himself for his results, so if the results of the Python code are consistent with Van der Eerden's results, the Python code is validated.

For validation, the result seen in Figure 2.12 in Section 2.2.5 is used. This result is useful for validation, as it also contains a QWT system combining in-series and in-parallel connected tubes, for which the Python code is also used. Of the three results in the figure, the result with $\alpha > 0.80$ is chosen and the corresponding measurements are given in Table 3.1.

Table 3.1: Geometric parameters for three coupled tubes (Van der Eerden, 2000)

Parameter	**Size**
Length main tube $[m]$	0.06
Length tube 1 $[m]$	0.054
Length tube 2 $[m]$	0.068
Diameter main tube $[m]$	0.01
Diameter tube 1 $[m]$	0.002
Diameter tube 2 $[m]$	0.0022
Porosity $[-]$	0.3

After entering the data of Table 3.1 in the Python code, the code produces the graph as shown in Figure 3.3.

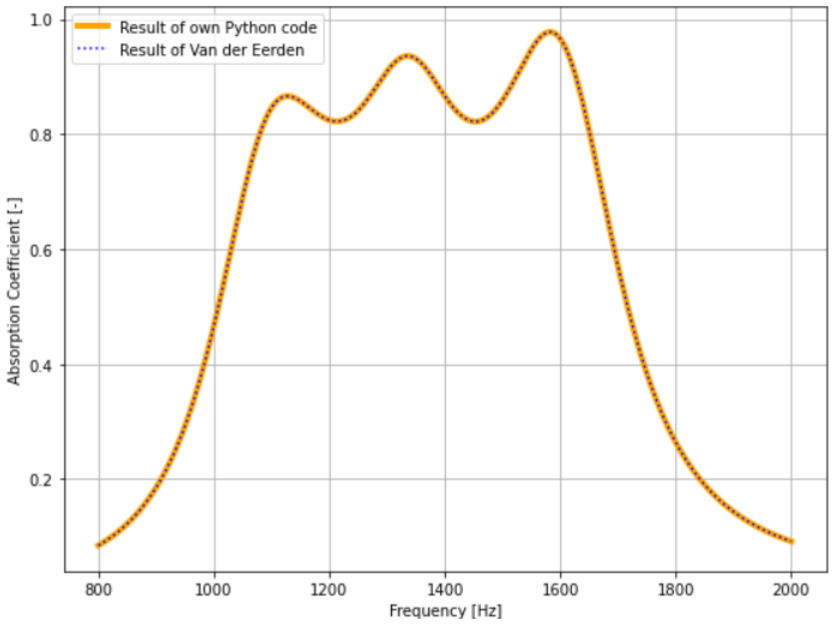

Figure 3.3: Own Python code for calculating absorption coefficients of a quarter-wavelength tube connected with two quarter-wavelength tubes compared to the same system calculated by Van der Eerden (Van der Eerden, 2000)

Comparison of the two graphs in Figure 3.3 shows that the Python code obtains the correct results.

In conclusion, the Python code including the recursive formulation (and DEAP) is able to calculate a correct QWT system.

3.2. Numerical analysis

To bridge the gap between the theory and real prototypes, the model will be simulated. The biggest advantage of a numerical model is that 3-dimensional phenomena can be incorporated much better, and the whole system can be calculated in more detail. However, the computation time is much longer, but it is still better than testing the prototype already without further detailed testing. For the simulations, the finite element analyser (or FEA-program) COMSOL Multiphysics, or COMSOL in short, will be used. COMSOL is an excellent program to couple different physical effects, such as acoustics, thermal effects, and viscous effects. For a system consisting of QWTs, this is ideal, as not many other FEA-programs are capable of doing so. The program is also used by Bezemer-Krijnen (2018), De Bie et al. (2022) and Carvalho de Sousa et al. (2021) for instance for the simulation of QWT systems. To determine the absorption coefficient per frequency of the model, an impedance tube setup is also modelled in front of the QWT system model. The setup of the impedance tube is described in Section 3.3.3, as the settings in COMSOL are the same as for the real impedance tube.

For the numerical analysis, the COMSOL setup will be elaborated in further detail first, and this will be followed by the verification and validation of the model. For the full set-up the manual of COMSOL Multiphysics (2018) is used.

3.2.1. Setup of the COMSOL model

COMSOL is an FEA program that is ideal for combining different kinds of physics. Moreover, COMSOL has its own specific acoustics module for fluids and solids. It is also possible to include material characteristics for, for instance, the walls of the QWTs. However, the effects of the material are mainly excluded, except for the impedance of the walls. The effect of the other characteristics will be tested during the experimental analysis.

The two most important physics interfaces in the acoustics module used for the QWTs model are ”Pressure Acoustics” and ”Thermoviscous Acoustics”. Pressure Acoustics physics will be used for the impedance tube and for the first simulation of the QWT system using the ”Narrow Region Acoustics” domain, while Thermoviscous Acoustics will be used for detailed simulations of the QWT system. Both physics will now be explained in more detail. All simulations are performed with a step size of 5 Hz, to limit computational cost.

Pressure Acoustics and the Narrow Region Acoustics domain

Pressure Acoustics, or more specifically Pressure Acoustics in the frequency domain (acpr), is a physics interface used to determine pressure variations due to acoustic waves and is useful when harmonic variations in the pressure field are present. The acpr physics interface solves the Helmholtz equation (Formula 2.9) for the given frequencies, so no viscothermal effects are considered. This is ideal for wide tubes, such as the impedance tube, which has an diameter of 0.10 m.

For the acpr interface, all geometry walls present in this interface are automatically sound hard boundary walls. This means that these walls have an infinite impedance, which is also the starting point of the Python code. The entrance of the impedance tube will have a Normal Acceleration boundary to impede sound waves with an acceleration of $1\ m/s^2$.

It is also possible in the acpr physics interface to assign the Narrow Region Acoustics fluid model to a certain geography. It is used by Carvalho de Sousa et al. (2021) for a model consisting of QWTs. With the Narrow Region Acoustics fluid model, it is possible to determine viscous and thermal losses in the viscothermal boundary layer in a QWT. It can be used for long tubes with equal cross sections. For circular ducts, the model uses the low-reduced frequency model, just as the code for the analytical analysis. This makes the two analyses very comparable, so in this way it can be evaluated to determine what the effect of a three-dimensional model is compared to code results. The exact calculation principles of this model can be found in the manual of COMSOL Multiphysics (2018).

With Pressure Acoustics applied to the impedance tube and the Narrow Region Acoustics fluid model applied to the QWT, the model will look as presented in Figure 3.4.

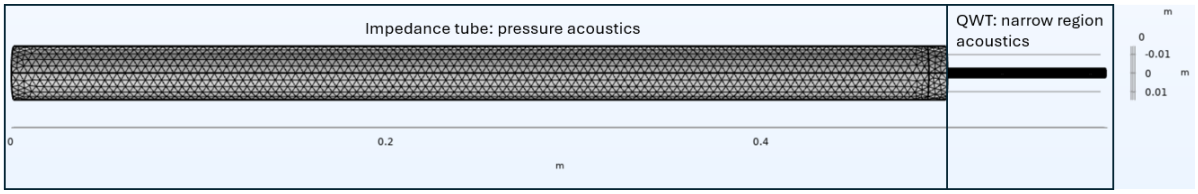

Figure 3.4: The model of a QWT connected to an impedance tube with corresponding Pressure Acoustics physics settings

As seen in the figure, the geography is meshed. For good practice, the mesh should have a size of at least 5-10 elements per wavelength. As the COMSOL model is simulated over a frequency band of 1600 Hz (the same as for impedance tube measurements), this means that the mesh size should be at most $\frac{343}{1600 \cdot 5} = 0.0429\ m$ for 5 elements per wavelength or $\frac{343}{1600 \cdot 10} = 0.0214\ m$ for 10 elements per wavelength. Therefore, the ”finer” setting is chosen in COMSOL, as this setting has a minimum element size of 0.0322 m. The mesh will have a free tetrahedral form.

Thermoviscous Acoustics

Although the Narrow Region Acoustic model is useful for comparison with the analytical analysis, the advantage of COMSOL is mainly that even more detailed three-dimensional calculations can be done of the QWT system. To do so, the Thermoviscous Acoustics interface is used. The Thermoviscous Acoustics interface, or Thermoviscous Acoustics in the frequency domain (ta), computes, in addition to acoustic variations of pressure, variations of velocity and temperature as well. Instead of the low-reduced frequency model, ta uses the linearized Navier-Stokes equations in quiescent background conditions solving the continuity, momentum and energy equations.

The length scale where ta is necessary depends on the viscous (δ_v) and thermal (δ_t) boundary layers. These layers can be calculated with the following formulas:

$$\delta_v = \sqrt{\frac{\mu}{\pi f \rho_0}} \tag{3.5}$$

$$\delta_t = \sqrt{\frac{k}{\pi f \rho_0 C_p}} \tag{3.6}$$

All variables in Formulas 3.5 and 3.6 are given in Section 2.2.1. The ratio of the viscous boundary layer and thermal boundary layer gives the square root of the Prandtl number (σ), which can also be calculated with Formula 2.19.

To correctly incorporate the viscous and boundary layers into the Thermoviscous Acoustics interface, a boundary layer mesh should be added to the general mesh. The general mesh should remain the same size as for Pressure Acoustics, as this is already fine enough for Thermoviscous Acoustics. The boundary layer will not consist of one layer with equal thickness as the viscous layer, as the viscous (and thermal) layer has effects on the pressure over a wider area than just the viscous layer thickness.For good practise, two different kind of meshing are possible:

- Using total thickness: The total thickness is used, which is calculated by multiplying the thickness of the viscous layer by the number of layers (4-6). COMSOL automatically calculates the thickness of each layer while also using a stretching factor (1.1-1.3), which makes each layer further away from the wall slightly thicker. These layers do not need to be as precise as the first layer.
- Using first layer thickness: the thickness of the first layer of the boundary layer is calculated by dividing the viscous layer by 5. The number of layers will be between 5 and 10 and the stretching factor is the same as for using the total thickness method.

For example, the viscous layer for 1600 Hz will be $55\ \mu m$. Using the total thickness method and choosing 4 layers, the total thickness will be $4 \cdot 55 = 220\ \mu m$. When using the first layer thickness method, the first layer will have a thickness of $\frac{55}{5} = 11\ \mu m$. Choosing 7 layers and considering a stretching factor

of 1.2, the total thickness will be $142\ \mu m$. This shows that both methods give quite different results if the settings are not adjusted to each other. For the numerical analysis, the first layer thickness method is used with aforementioned settings.

The Thermoviscous Acoustics interface will only replace the Narrow Region Acoustics domain, which is assigned to the QWT system. The impedance tube is still modelled with Pressure Acoustics physics. The setup can be seen in Figure 3.5.

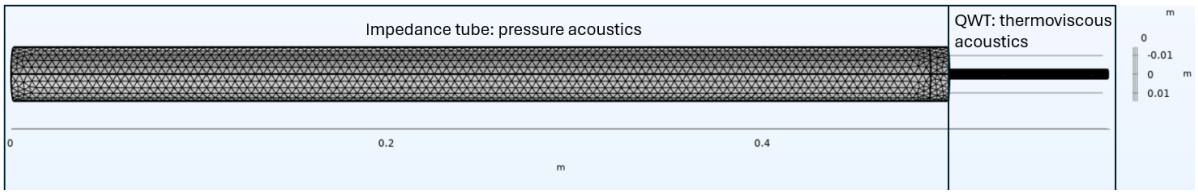

Figure 3.5: The model of a QWT connected to an impedance tube with corresponding Pressure Acoustics and Thermoviscous Acoustics physics settings

It should be noted that it is also possible to apply impedance boundaries for the QWTs. This could be useful in mimicking the material the model is made of for the experimental analysis. For this analysis, the material will be PLA (see Section 3.3.2) with an impedance between $2.6 \cdot 10^6$ and $2.8 \cdot 10^6$ (Parker et al., 2010) for PLA with an infill and thickness sufficiently high. Python tests indicate that these impedance values are high enough to consider the wall as Sound Hard Wall.

3.2.2. Verification and validation of numerical method

To verify and validate the COMSOL model which is used for the numerical analysis, the same procedure is used as for the verification and validation of the analytical analysis (see Section 3.1.3. This means that for verification, a tube with a length corresponding to the absorption of 1000 Hz with different diameters is used. For validation, a QWT system consisting of one main tube and two smaller tubes is used as proposed by Van der Eerden (2000).

Verification of numerical method

For the verification of the COMSOL model, the Pressure Acoustics model in combination with the Narrow Region Acoustics domain or in combination with Thermoviscous Acoustics physics are taken into account. The procedure is the same as for the verification of the analytical method, which means that one QWT with a length of 0.086 is considered. In addition, the same three different diameters are considered, namely 0.005, 0.01 and 0.05 m. To achieve a porosity of 0.03, the cross section of the impedance tube is adjusted. This means that the impedance will have diameters of 0.0289, 0.0577 and 0.289 m.

In addition, the dimensions of the impedance tube should be changed for different diameters compared to the set-up explained in Section 3.3.3. The distance between the first microphone and the sample should be the same as the diameter of the impedance tube, and the distance between the speaker and the second microphone should be 3 times its diameter (International Organization for Standardization, 2023). However, the distance between the two microphones to determine the sound pressures depends on the ”maximal frequency”. This maximal frequency is dependent on the diameter of the impedance tube, as for wider diameters, non-planar waves will occur for lower frequencies. The maximum frequency is calculated with $f_u \cdot d < 0.58 \cdot c_0$. This formula gives problems for an impedance tube diameter of 0.289 m, as the corresponding maximal frequency is 688 Hz. In Section 3.1.3, it can be seen that the absorption peak for this diameter is 801 Hz. This is higher than the aforementioned 688 Hz, so results for this diameter will be less accurate for verification. The spacing between the two microphones is calculated with $f_u \cdot s < 0.45 \cdot c_0$.

Taking into account these minimal and maximal dimensions, the chosen dimensions are given in Table 3.2.

Table 3.2: Different determined dimensions for different impedance tube diameters

Diameter [m]	Distance sample - first microphone [m]	Distance between microphones [m]	Distance second microphone - speaker [m]
0.0289	0.03	0.02	0.10
0.0577	0.06	0.04	0.20
0.289	0.30	0.10	0.90

First, the three different QWTs are verified using Narrow Region Acoustics. The result of the simulation with COMSOL compared to the Python results can be seen in Figure 3.6.

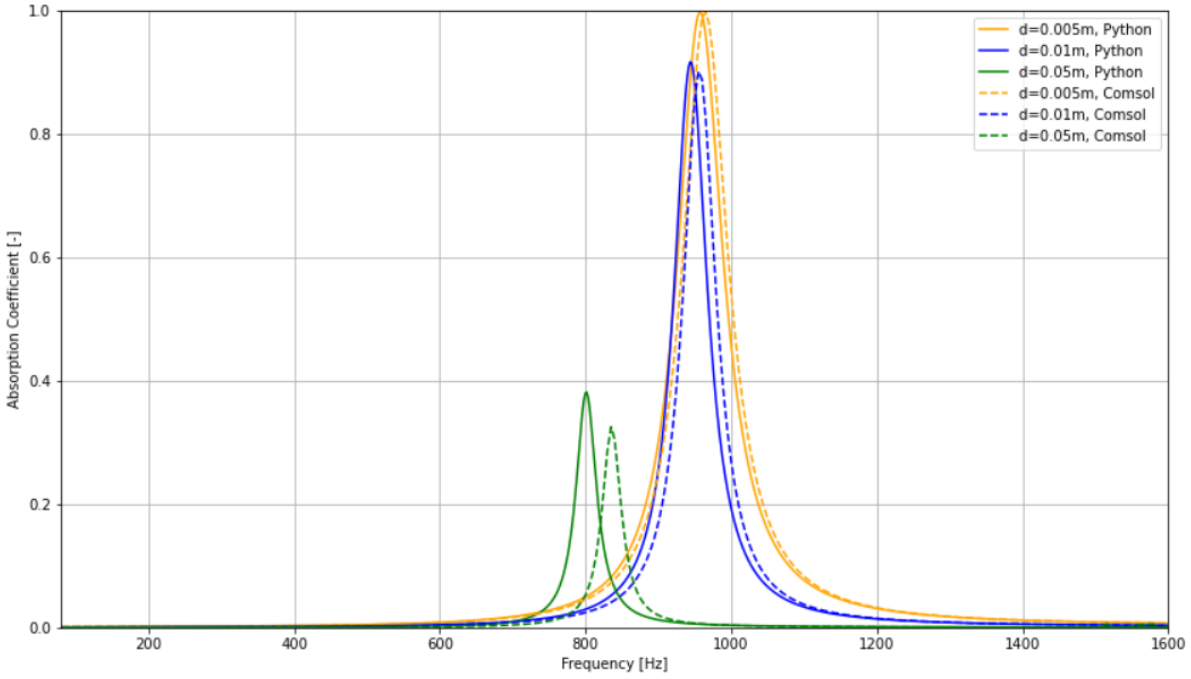

Figure 3.6: Absorption coefficients for a with COMSOL and Python simulated QWT with $L = 0.086$ and $\Omega = 0.03$ for three different cross sections

The three absorption peaks of the COMSOL simulation for three different cross sections are $835\ Hz$ for $d = 0.05\ m$, $955\ Hz$ for $d = 0.01\ m$, and $965\ Hz$ for $d = 0.005\ m$. Compared to the results of Python, which are, respectively, 801, 943 and 957 Hz, the results do align more for higher frequencies than for lower frequencies. These results verify that the COMSOL simulation with the biggest impedance tube cross section is indeed off due to the occurrence of non-planar waves. To further verify this, the Python code shall also be compared to the COMSOL simulation using Thermoviscous Acoustics physics. The comparison between the Narrow Region Acoustics results and Thermoviscous Acoustics results in COMSOL can be seen in Figure 3.7.

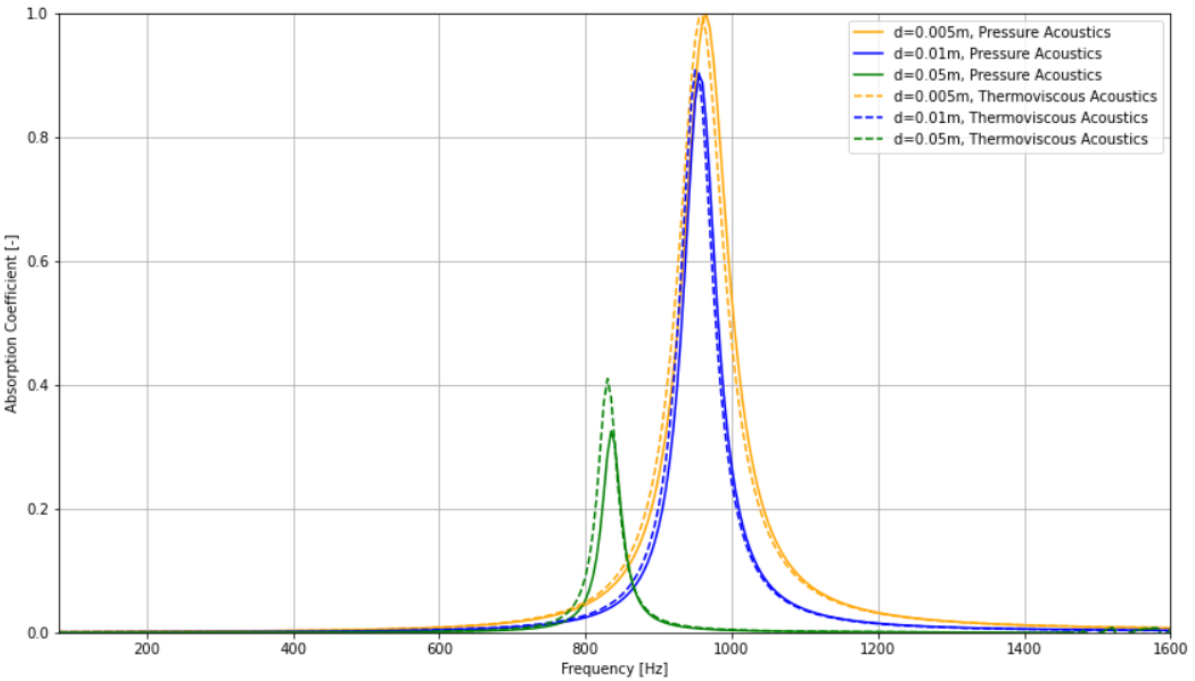

Figure 3.7: Absorption coefficients for a with Narrow Region Acoustics and Thermoviscous Acoustics simulated QWT with $L = 0.086$ and $\Omega = 0.03$ for three different cross sections

The results in Figure 3.7 show that simulation using Narrow Region Acoustics or Thermoviscous Acoustics results in almost the same results. The only small differences are that the absorption is higher for Thermoviscous Acoustics for lower frequencies and for all results a very small negligible shift of resonance frequencies to lower frequencies. The difference between these two kinds of physics will also be compared in the validation. If the differences stay negligible in the validation, then only Narrow Region Acoustics will be used for the final model. The reason for this is its lower computational cost.

Validation of numerical method

To validate the numerical method, the same approach is used as for the validation of the analytical method. This means that the numerical results, both with the use of Narrow Region Acoustics or Thermoviscous Acoustics, are compared to the results of a QWT system of Van der Eerden (2000). The data and corresponding results are given in Table 3.1 and Figure 2.2.5. The only difference is that the porosity is changed, due to the fact that the impedance tube has the same cross section for validation as a real impedance tube ($d = 10\ cm$). This will cause the porosity to be 0.01. The result is presented in Figure 3.8.

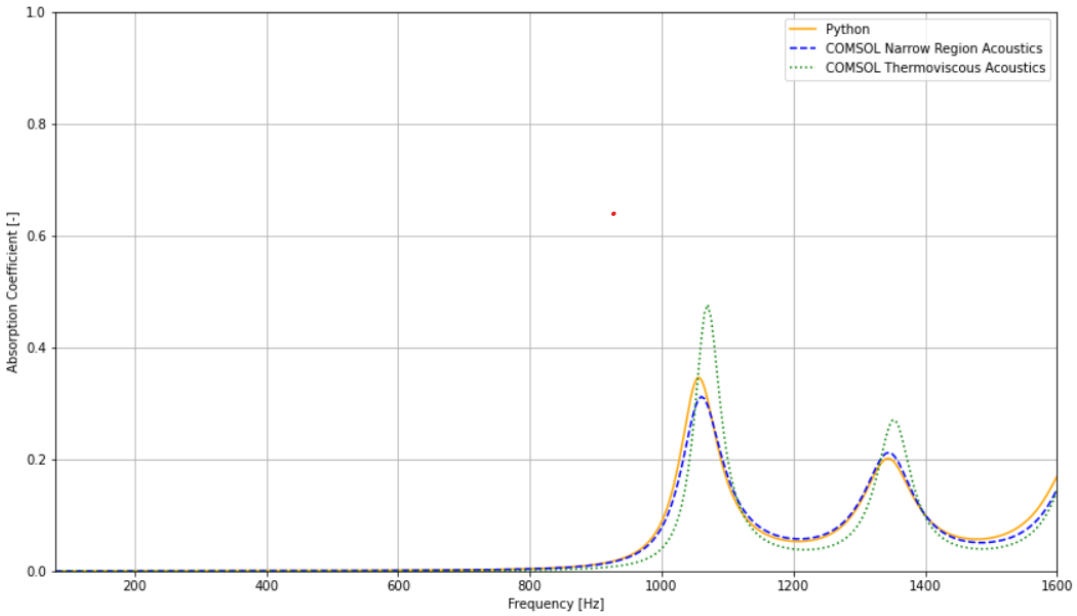

Figure 3.8: Absorption coefficients for a QWT system model with the use of Python and two different COMSOL models

The results in Figure 3.8 show exactly the results as expected: the results of the COMSOL simulation using Narrow Region Acoustics and the Python code are almost the same, while the COMSOL simulation using Thermoviscous Acoustics contains higher absorption peaks. The result validates that the COMSOL models for numerical analysis give the correct results.

3.3. Experimental analysis

The goal of the experimental analysis is to obtain the physical results of the QWT system determined during the analytical analysis. Physical test pieces are obtained by 3D printing the QWT system, which have the goal to show if the results obtained from the analytical and numerical analyses are in accordance with actual physical results. For the experimental analysis, three steps are needed: modelling the QWT system in a three-dimensional modelling program to get a system that fits in the test area, 3D printing of the model of the QWT system, and testing with an impedance tube to get the actual absorption coefficients of the studied frequency range. The test area for the 3D printed QWT system is therefore also the impedance tube. The modelling will be done with Rhino 3D using its Grasshopper plug-in, and will be initially explained in this section. Afterwards, the 3D printer setup will be elaborated using the Ultimaker S5 printer, followed up with the working principles of the impedance tube. Finally, the aforementioned method will be verified and validated.

3.3.1. Rhino 3D model

To obtain an actual physical test model of the calculated QWT system, Rhino 3D is used. Rhino 3D is a modelling program in which it is possible to change the dimensions and characteristics of the model parametrically using its Grasshopper plug-in. This makes a change of length, diameter, and orientation of a tube in the system much easier.

For the model, two physical limits are considered that are based on the dimensions of the impedance tube in which the model will be tested, namely:

- The system cannot have a width that is bigger than 10 cm, as this is the diameter of the cross-section of the impedance tube.
- The system cannot have a height that is higher than 20 cm, as this is the height of the impedance tube.

The model is made in a clear stepwise way: First, the main tube is made without any form of bending with the connected tubes attached to it (see Figure 3.9). For these tubes, it is possible to change the

height, diameter, and thickness.

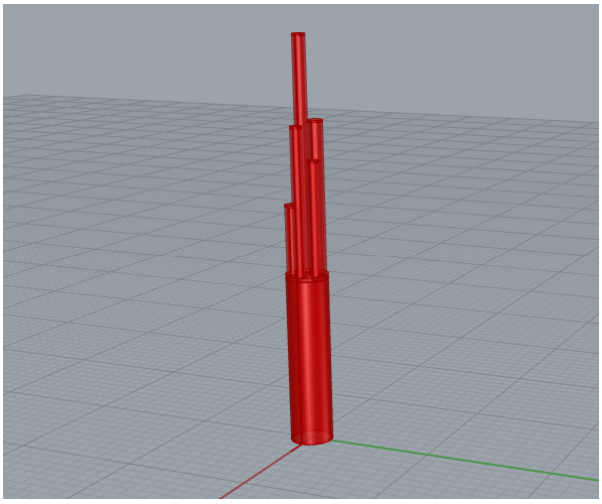

Figure 3.9: A straight main tube connected with five straight connected tubes. Dimensions are chosen randomly for the sake of example.

The connected tubes are placed at the edge of a circle that lies within the cross section of the main tube. It is possible to change the diameter of this circle and so of the distance between the centre of the main tube and the centre of the connected tubes.

Afterwards, a bended line is made that the straight tube system will follow (see Figure 3.10a). The variables for this bended path are the radius of the spiral and the radius of the first bend around the horizontal axis. As the height of the upward moving spiral is completely based on the diameter and thickness of the walls of the main tube, the main tube will be adjacent to the tube walls one full turn above and underneath it (see Figure 3.10b).

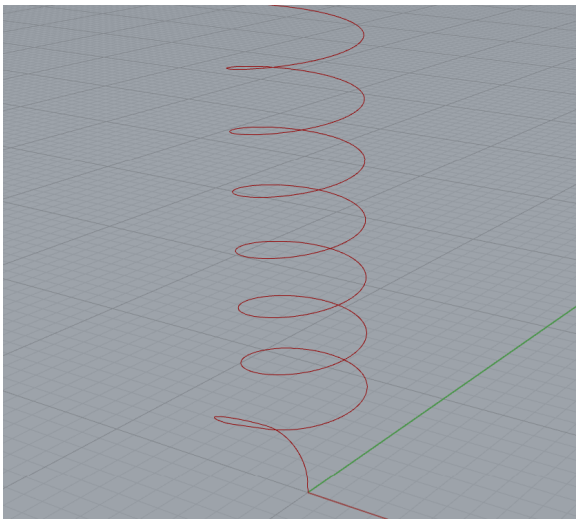

(a) The bending pattern

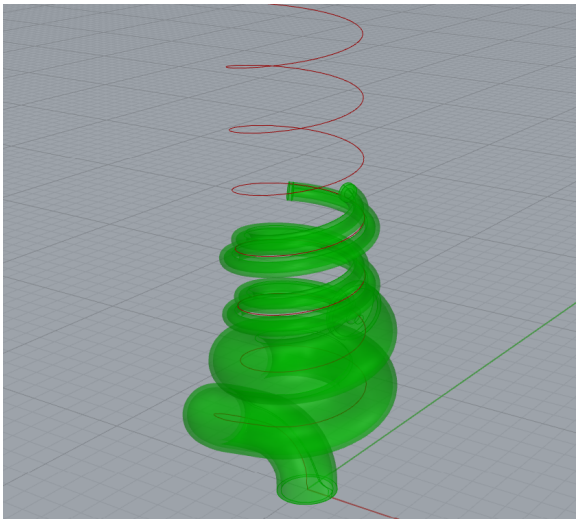

(b) The tube actually following the bending pattern. Dimensions are chosen randomly for the sake of example.

Figure 3.10: Bending pattern and its physical realization in Rhino 3D

The thickness of the walls was not needed for the analytical and numerical analyses. However, the printed model needs a thickness as sound waves will otherwise be transmitted through the walls of the tube. The thickness of these walls, based on the material of the printed system, will be explained in Section 3.3.2.

After this step, only the casing of the system needs to be made. This casing is needed, as air should not flow near the opening of the system. The casing will consist of a bottom with the opening of the QWT system in it, and walls with the same height as the QWT system (see Figure 3.11. The walls of the casing will be thicker than the walls of the QWT system.

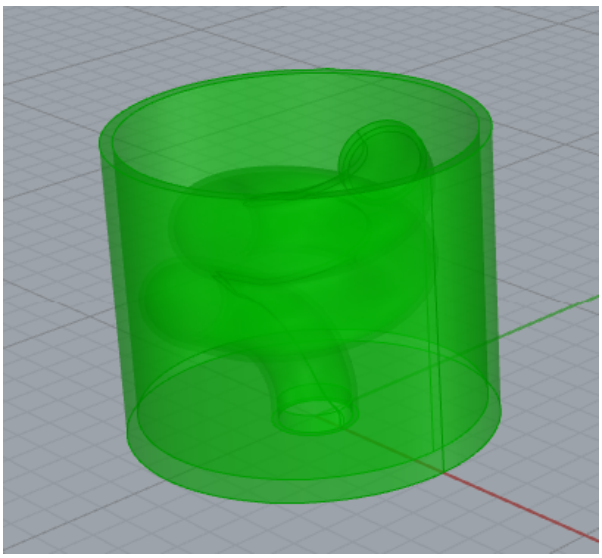

Figure 3.11: The casing of the QWT system in Rhino 3D

When the model of the QWT system and the casing are sufficient within its imposed limits, the model only needs to be meshed and uploaded to a 3D printing program.

3.3.2. 3D printing of the model

To perform physical tests with the model, the model should first be made physical. This is done using a 3D printer. 3D printing, or additive manufacturing, is done by using an Ultimaker S5 printer, which is present at the Faculty of Civil Engineering and Geosciences in Delft (see Figure 3.12). The Ultimaker S5 uses Fused Deposition Modelling (FDM), which means that printed parts are built layer by layer by melting material filament. FDM is relatively cheap, has many usable materials available and is easy to use (Kafle et al., 2021). These advantages are in contrast to other printing options such as Stereolithography (SLA) and Selective Laser Sintering (SLS). However, SLA has higher precision and a smoother surface finish, while SLS does not need to have support structures for overhanging parts. The main reason for choosing an FDM 3D printer is that it is already available at the Faculty of Civil Engineering and Geosciences, as mentioned beforehand.

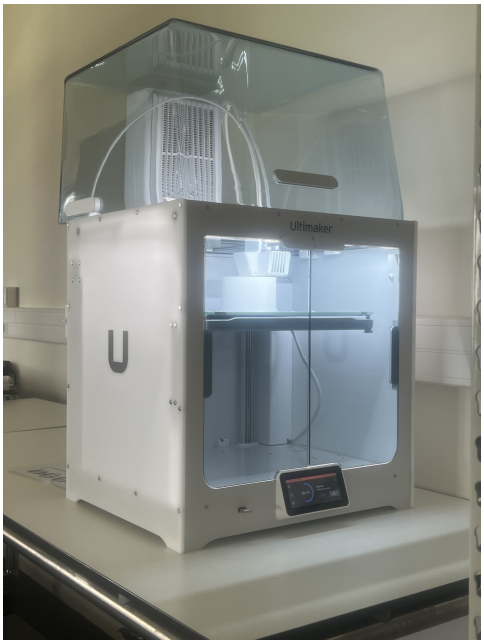

Figure 3.12: The Ultimaker S5 3D printer

Another advantage of an Ultimaker S5 printer is that it contains a dual extruder. The dual extruder makes it possible to print two different kinds of materials. For the model of a QWT system, two kinds of materials are needed: PLA and PVA. PLA (Poly-Lactic Acid) is the main material for the model. Its advantages are that PLA is easily printable with relatively low printing temperatures (180-220 $^{\circ}C$), has an excellent surface finish and adhesion, and is biodegradable ((Pang et al., 2010). In addition, it is an affordable material and has very low shrinkage during cooling. However, it is a brittle material, so this should be kept in mind. Polyvinyl alcohol (PVA) is used as a support material for overhangs in the model. The big advantage of PVA as a support material is that it is water soluble: The model can be placed in water to remove (dissolve) the supports (Ng et al., 2022). When dissolved in water, the solution does not have any negative environmental effects, as it is still biodegradable. To ensure that all PVA is solved, the print is placed in water for 24 hours.

In contrast to other analyses, the wall thickness of the tubes should be taken into account. The thickness of a tube with 100% infill does not have an influence on sound absorption when it is above 1.4 mm (Catapane, Petrone et al., 2023). As the nozzle size of the printer is 0.4 mm, a multiple of this value is chosen. Therefore, the wall thickness of all tubes is 1.6 mm. To prevent any form of incoming waves into the casing, the wall thickness of the casing is set as 5 mm.

The Rhino-made model, as described in 3.3.1, is imported in the Ultimaker Cura slicing application, in which the model is prepared for additive manufacturing. The complete settings for the printing of the models are included in Appendix C. First, some test prints are printed to experience the consequences of different printing settings. Afterward, test pieces containing just one QWT are printed to see if the test pieces actually absorb the associated frequency. When these are sufficient, a validation model is 3D printed, and if the measured results are comparable with the original results, the QWTs system as determined in the analytical analysis is 3D printed.

3.3.3. Impedance tube

For actual measurements of the 3D printed model, an impedance tube will be used. Impedance tube measurements are the most convenient and standard manners for doing acoustic measurements (Van der Eerden, 2000). For the measurements of this thesis, the Brüel & Kjær 4206 impedance tube present at the Faculty of Architecture and the Built Environment will be used. When an impedance tube is used, normal incident waves are considered. This should be considered because oblique incoming sound waves will result in different absorption coefficients. The main principle of an impedance tube is simple: a loudspeaker at one end of the tube will produce a sound which is reflected by the test sample at

the other end of the tube. In the impedance tube, a standing wave pattern will occur, consisting of the forward moving and reflected wave. In the impedance tube, two microphones are placed, making it possible to calculate a transfer function. The technique using two fixed microphones is also called the 2p method.

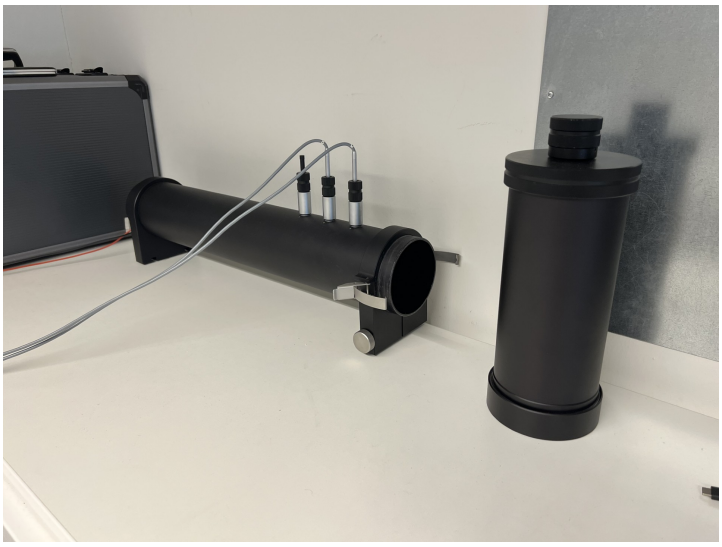

Figure 3.13: The Brüel & Kjær 4206 impedance tube present at the Faculty of Architecture and the Built Environment. A sample will be put in the right tube and connected to the left tube.

For the impedance tube present at the Faculty of Architecture and the Built Environment, the microphones are separated by 0.05 metres. When using an impedance tube, the microphones are initially calibrated to determine phase and gain characteristics. In addition, the impedance tube has a diameter of 10 centimetres, and a maximal sample height of 20 centimetres, which limits the size of the test sample. The transfer function of the two microphones can be written as $H_{2p} = \frac{p_2}{p_1}$, with p_1 and p_2 the pressures in the frequency domain measured at each microphone. When this transfer function is calculated, the reflection coefficient of the system can be calculated using the following formula:

$$R(x = L) = \frac{H_{2p} - e^{-\Gamma k x_2}}{-H_{2p} + e^{\Gamma k x_2}} \cdot \frac{e^{\Gamma k L}}{e^{-\Gamma k x_2}} \tag{3.7}$$

In this formula, x_2 is the distance between the two microphones and L is the position of the sample towards the loudspeaker. When this reflection coefficient is calculated, the absorption coefficient can be calculated with Formula 2.8. This process is completely based on the standard NEN-EN-ISO 10534-2:2023 (International Organization for Standardization, 2023).

3.3.4. Verification and validation of experimental method

For the final result of this research, it is very important that the printed test models are verified and validated. These models should prove that the designed system actually absorbs sound as calculated with theory, so unreliable results are very detrimental for the proof of the theory. To verify the model, a 8 cm high tube is printed in straight and bended form. For the validation, the same model as used for validation of the analytical and numerical methods is used.

Verification of the experimental method

For the verification of the printed models, a tube with a length 8 cm is used, to make it more exactly accurate to 3D print. In addition, only one diameter is now considered with one corresponding porosity as the diameter of the impedance tube is fixed (10 cm), in contrast to the COMSOL model. The diameter of the printed model will be 1 cm with a corresponding porosity of 0.01.

As the effect of bending the tube is not yet considered except for theory, the same proposed verification model is also printed with a bended tube. The two different verification models can be seen in Figure 3.14.

Figure 3.14: One bended and one straight 3D printed QWT with casing. $L = 0.08\ m$ and $d = 0.01\ m$. 150 ml coffee cup for indication of scale. Masking tape applied to ensure casing fits exactly in impedance tube

The results of the straight and bended printed models in comparison to Python results can be seen in Figure 3.15.

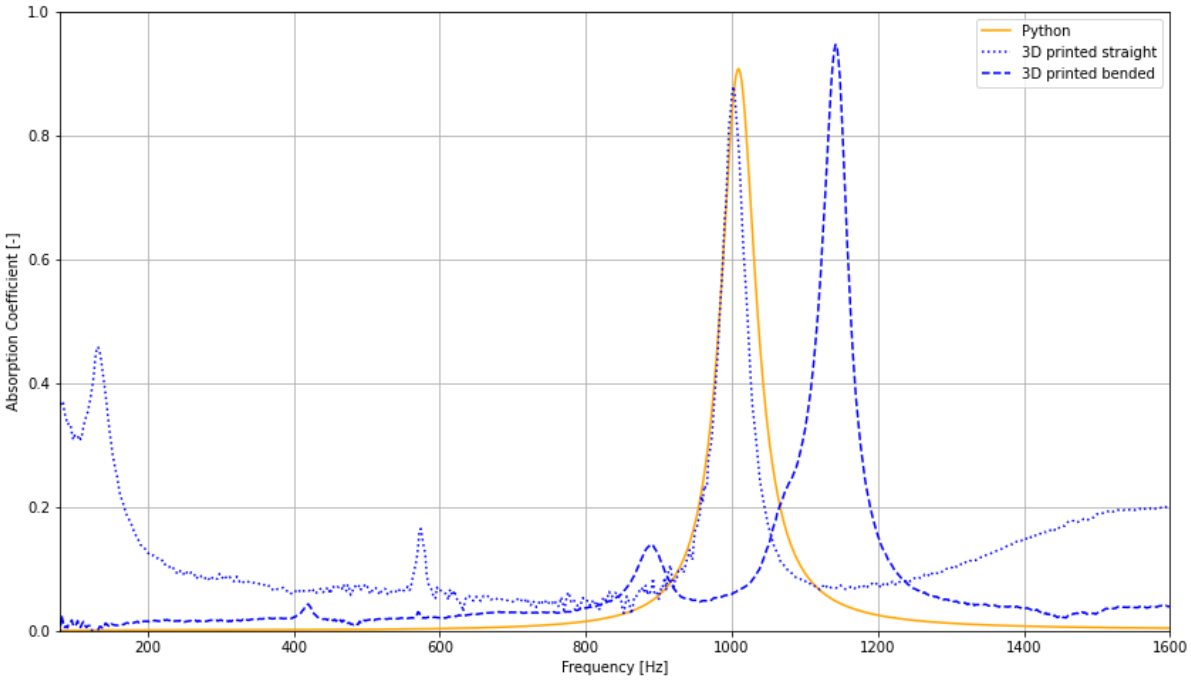

Figure 3.15: Absorption coefficients of a Python calculated, 3D printed straight, and 3D printed bended QWT. $L = 0.08\ m$ and $d = 0.01\ m$

The result is compared with the Python result instead of the COMSOL result, as both results are very similar. The Python graph and the 3D printed straight graph align very closely (1002 and 1008 Hz). However, the bended tube has a big shift towards higher frequencies. The shift of the resonance frequency and the gain of the absorption is as expected (Cambonie et al., 2018), but the shift is even

more than just 1-2% of the resonance frequency. A possible explanation for this could be that the PVA inside the QWT is not completely dissolved, so the length in the tube is shorter, which causes higher resonance frequencies. Except of this higher shift, the printed models verify the theory.

Validation of the experimental method

To validate the 3D printed model, the same validation method is used as for the analytical method and the numerical method: comparison to a QWT system result of Van der Eerden (2000). The verification shows that a shift of the resonance frequency to higher frequencies can be expected with an increase of the absorption. However, the effect of a QWT system consisting of in-series and in-parallel connected tubes is yet unknown. The 3D printed of the model of Van der Eerden (for the data, see Table 3.1) can be seen in Figure

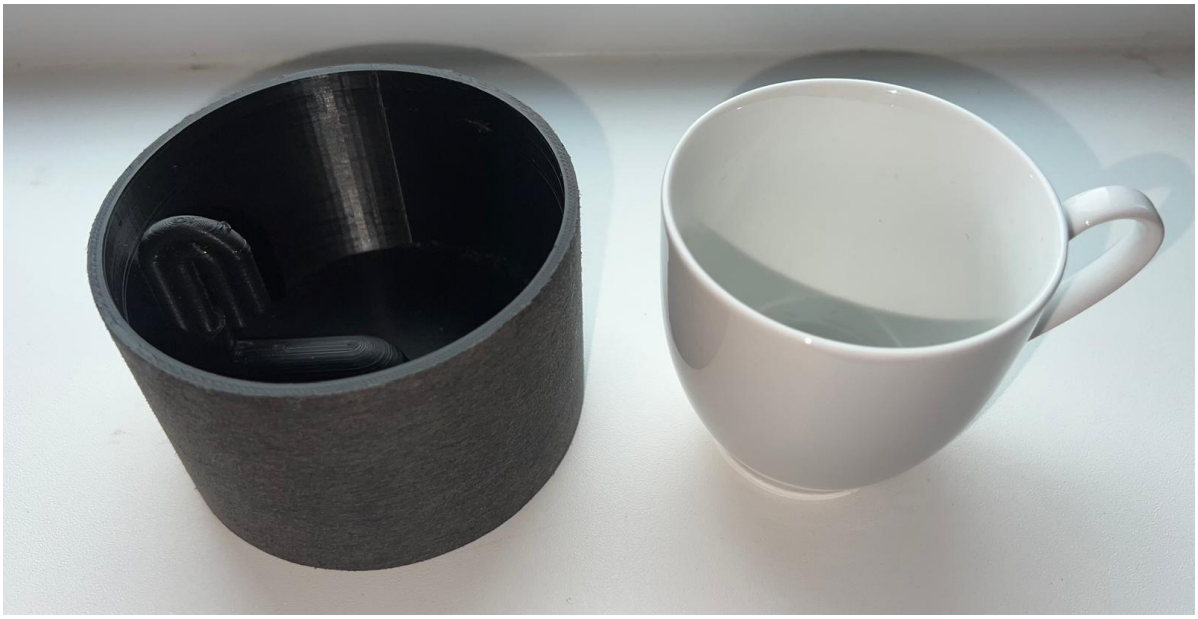

Figure 3.16: One main QWT connected with two in parallel placed QWTs. 150 ml coffee cup for indication of scale. The side of the casing is sanded to fit the impedance tube exactly

The results of the printed model compared to the Python result for the same model can be seen in Figure 3.17. It must be noted that the Python graph differs to earlier validations, as the porosity is different. The reason for a different porosity is the fixed size of the impedance tube.

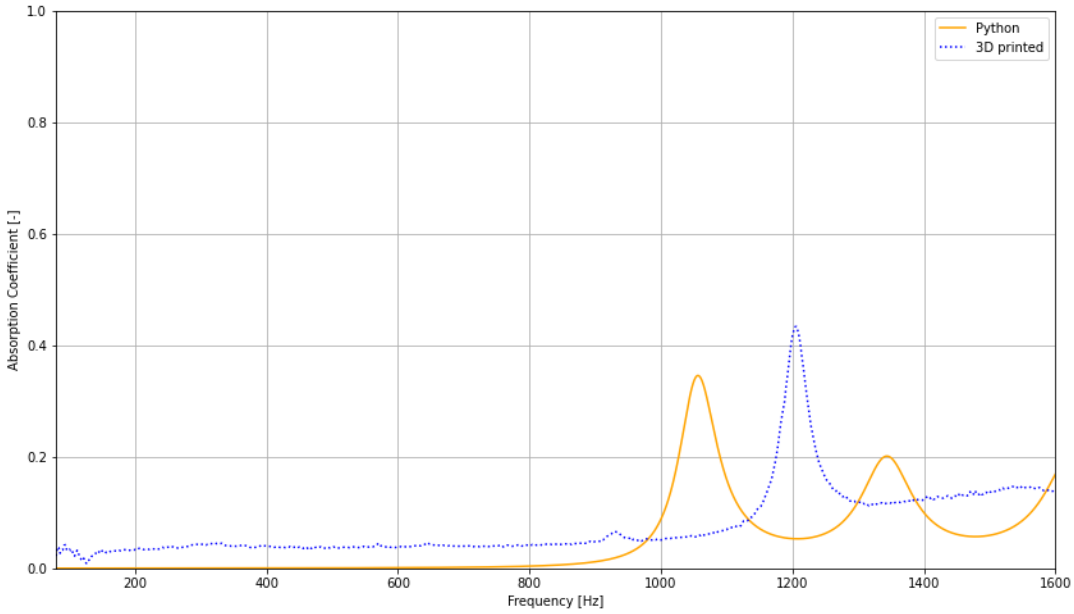

Figure 3.17: Absorption coefficients of a Python calculated and 3D printed QWT system

The main peak shift of the 3D printed result corresponds slightly to the theory of bended tubes: a shift of the resonance frequency to a higher frequency by approximately 10% instead of 1-2%, but also a higher maximum absorption coefficient. The larger increase may be due to PVA that is still present in the tubes, just like for the verification. In addition, the other peaks of the Python result can not be seen in the printed result. One of the possible reasons for this result is that the other peaks are also shifted to higher resonance frequencies, but they do not fit the frequency bandwidth of the impedance tube. However, in the result, some form of an upward opening parabola should be present, which is not the case. Another option is that the PVA in the two smaller QWTs is not dissolved. When the two QWTs are turned off in the Python code, the result in Figure 3.18 appears.

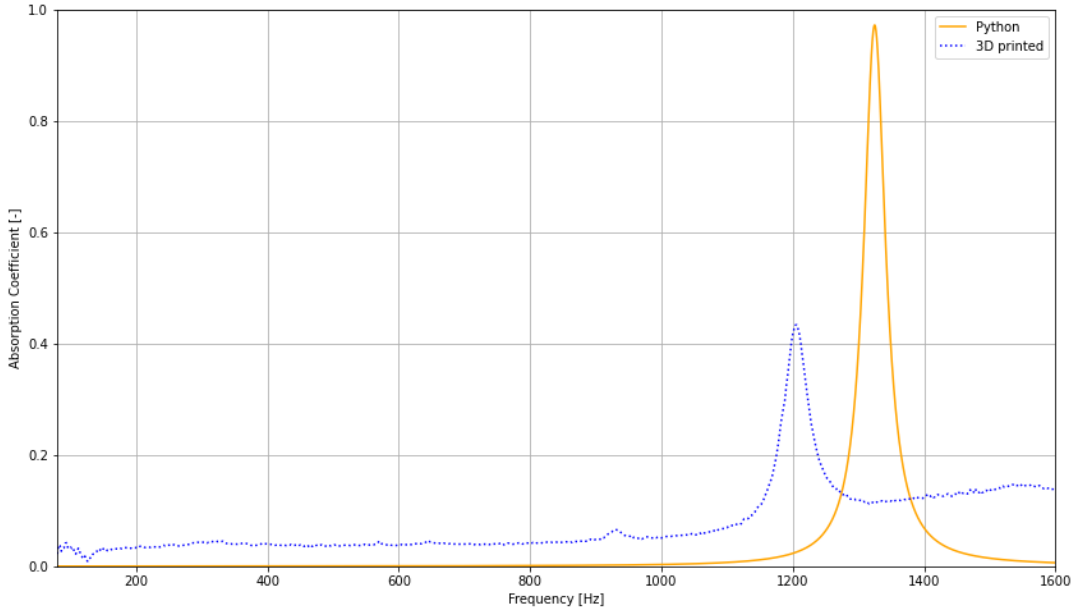

Figure 3.18: Absorption coefficients of a Python calculated and 3D printed QWT system, while the printed system contains to in-series connected QWTs

The result in Figure 3.18 shows that the two smaller QWTs are actually working in the printed model,

as the adjusted Python result does not match in the slightest. In conclusion, the peaks for higher frequencies disappear in the printed model. This is most likely due to bending effects and material imperfections. This should be considered for the final result.

4

Results

In this chapter, the goal of the research is tried to be obtained by using the aforementioned methods: designing an optimized QWT system consisting of in-series and in-parallel connected QWTs for low frequencies. First, the analytical results of the optimization procedure using the recursive formulation and DEAP are described. This is followed by the numerical results of COMSOL using Pressure Acoustics in combination with Narrow Region Acoustics. With the results of these analyses, the optimized model is 3D printed and tested with an impedance tube. If all results are sufficient, an optimized QWT system can be proposed for the absorption of low frequencies.

4.1. Analytical results

For the analytical analysis, a procedure is followed to have absorption as high as possible over the whole considered frequency band (88-355 Hz). The analytical analysis is used to answer the following sub-question:

- For which configurations does the system reach the maximum absorption?

The process of improvements of the optimization code is first described. This is done by considering different optimization objective definitions. After this process, the final result of the analytical analysis is described.

4.1.1. Testing of different optimization objective definitions

To obtain an optimization code that gives an optimized system with high absorption over the bandwidth and a small volume, the code should be developed. For instance, many different definitions of maximal absorption over the bandwidth exist. The absorption graph could have as high as possible peaks, but otherwise very low absorption. Another option is to have an as high as possible average absorption over the bandwidth. Therefore, different optimization objectives need to be tested. For these different objectives, the minimum and maximum dimensions for the length and diameters of the tube are as mentioned in the methods (see Section 3.1.2). Besides, the connected tubes can not have an bigger cross sectional area altogether than the area of the main tube. To secure this, the summed cross sectional area is multiplied with 0.8 for now. For the sake of developing the optimization, only a maximum of two connected tubes is considered during the progress.

Absorption with maximizing Area Under Curve

Initially, the optimization consisting of the maximization of absorption and the minimization of volume is performed by using the area under curve (AUC) method. By maximizing the area under the absorption curve, it was thought that maximal absorption could be achieved over the whole bandwidth. The first result, with the curve maximized over the whole bandwidth, can be seen in figure 4.1. Table 4.1 contains the dimensions of the tube.

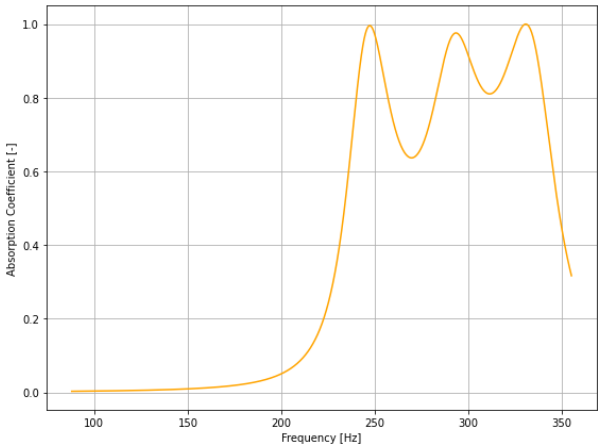

Figure 4.1: Maximizing AUC over whole frequency band

Table 4.1: Tube lengths and diameters for maximizing AUC over whole frequency band

Parameter	**Whole frequency band**
Length main tube $[m]$	0.276
Length tube 1 $[m]$	0.315
Length tube 2 $[m]$	0.260
Diameter main tube $[m]$	0.038
Diameter tube 1 $[m]$	0.006
Diameter tube 2 $[m]$	0.005
Volume $[m^3]$	0.000322

It can be seen in figure 4.1 that the curve is concentrated on the right side of the bandwidth. This is an obvious result, as absorption of higher frequencies requires less volume. In an attempt to spread the result more over the bandwidth, an AUC optimization is done per octave-band and one-third-octave band. For each band, the absorption is maximized. This changes the maximization into a multi-objective maximization, as each octave band is maximized independently. The results can be seen in figure 4.2a for the octave-band division and in figure 4.2b for the one-third octave-band division. The dimensions are summarised in table 4.2.

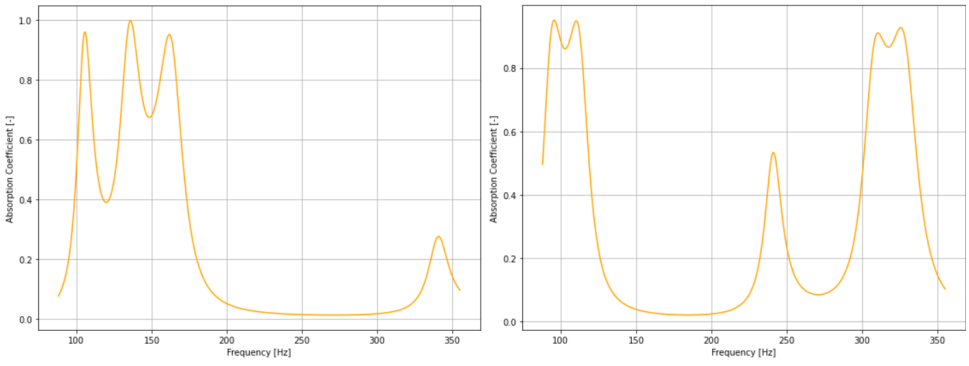

(a) Maximizing AUC over octave-bands **(b)** Maximizing AUC over one-third octave-bands

Figure 4.2: Maximizing AUC over different bandwidths

Table 4.2: Tube lengths and diameters for maximizing AUC over octave and one-third octave bands

Parameter	Octave bands	One-third octave bands
Length main tube [m]	0.577	0.791
Length tube 1 [m]	0.733	0.341
Length tube 2 [m]	0.557	0.796
Diameter main tube [m]	0.038	0.041
Diameter tube 1 [m]	0.008	0.008
Diameter tube 2 [m]	0.007	0.007
Volume [m^3]	0.000699	0.001073

These figures show a huge shift of the curve to the left. For the AUC-maximizing over the octave bands, only one octave-band is well maximized (with central frequency 125 Hz), as the other band is left behind. For AUC maximizing over six frequency bands, a large gap can be seen between a high peak at the left side of the figure and a smaller area at the right side of the figure. These results are not desired, as absorption over the whole area is still not achieved. In addition, volume usage increases heavily in comparison to maximizing AUC over the whole bandwidth, which is not desirable.

Maximizing of absorption average

The second method to try to increase absorption in a wider range is to maximize the average absorption over the whole bandwidth. In contrast to maximizing the AUC, maximizing the average avoids giving a preference to high small peaks when still very low absorption parts are present.

The initial result, with the maximizing of the average over the whole bandwidth, is presented in figure 4.3. Table 4.3 shows the dimensions for this result. In

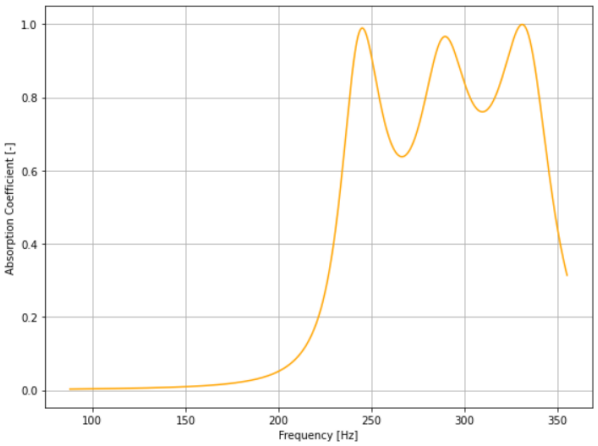

Figure 4.3: Maximizing average over whole frequency band

Table 4.3: Tube lengths and diameters for maximizing average over whole frequency band

Parameter	Whole frequency band
Length main tube [m]	0.275
Length tube 1 [m]	0.261
Length tube 2 [m]	0.321
Diameter main tube [m]	0.037
Diameter tube 1 [m]	0.005
Diameter tube 2 [m]	0.005
Volume [m^3]	0.000307

The result looks very much the same as the result in Figure 4.1, except that the right minimum in the absorption area is lower when using the average method than when using the AUC method. This method uses even slightly more volume (15 cm^3, so it is almost negligible). This result may be due to the randomness of the Python optimization code.

The same procedure is now followed for the average maximizing method as for the AUC-maximizing method, so optimization is also done for the frequency bandwidth divided in octave and one-third octave bands. These results are presented in Figures 4.4a and 4.4b.

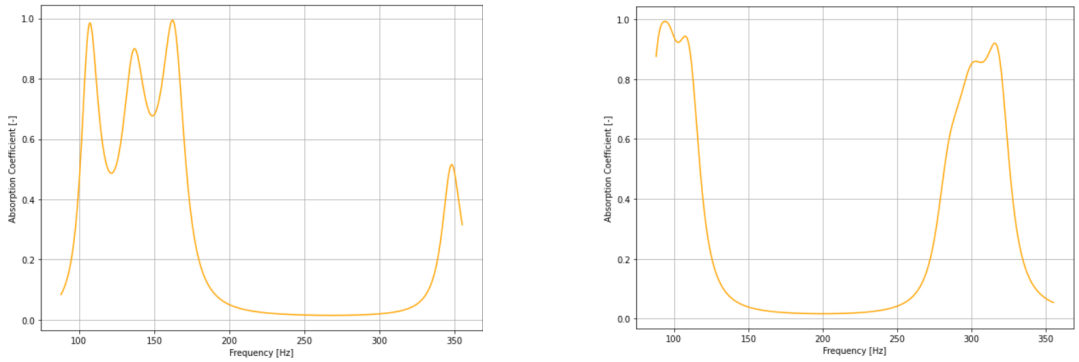

(a) Average and two bands

(b) Average and six bands

Figure 4.4: Absorption averaging method over different number of bandwidths

Table 4.4: Tube lengths and diameters for maximizing average over octave and one-third octave bands

Parameter	Octave bands	One-third octave bands
Length main tube [m]	0.601	0.828
Length tube 1 [m]	0.539	0.799
Length tube 2 [m]	0.717	0.867
Diameter main tube [m]	0.042	0.047
Diameter tube 1 [m]	0.007	0.007
Diameter tube 2 [m]	0.009	0.005
Volume [m^3]	0.000910	0.001462

The results look very much the same as the results of the AUC-maximizing. The only difference is that the volume use of average maximizing over the octave bands is bigger than for AUC-maximizing. In conclusion, taking the average (or multiple averages) of the absorption curve has had little to no effect on the increase of absorption.

Absorption with maximizing average of averages

The next improvement made is to take the average of the averages of the one-third octave band division. For each octave band, the average is determined and the average of all these octave band averages is calculated. Then, this average is tried to be maximized. The idea is that the maximization will be less localized and more equally spread. The result is presented in figure 4.5 and table 4.5.

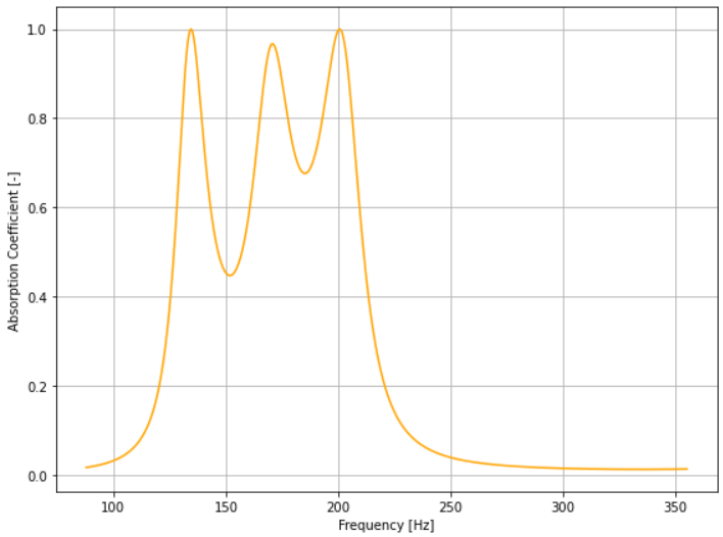

Figure 4.5: Maximizing average of averages of one-third octave bands absorption

Table 4.5: Tube lengths and diameters for maximizing average of averages of one-third octave bands absorption

Parameter	Value
Length main tube [m]	0.479
Length tube 1 [m]	0.571
Length tube 2 [m]	0.436
Diameter main tube [m]	0.038
Diameter tube 1 [m]	0.008
Diameter tube 2 [m]	0.0076
Volume [m^3]	0.000580

These are the first results which show a central wide absorption span while still having high peaks. In addition, volume usage is much lower for this result than for the results mentioned before. However, the absorption span is still not optimal, as the absorption above around 250 Hz is still close to zero. However, this result is promising and is the basis for final adjustments.

4.1.2. Final result

For the final definition of the objective functions, a greater variation of connected tubes is also considered. This is done as a possibility to broaden the absorption area even more. In addition, the standard-deviation of the six bandwidths is minimized. The idea behind this addition is that the difference in the absorption peaks and gaps will be lower, so a wider equal absorption span is achieved. This result is presented in figure 4.6 with the dimensions in table 4.6.

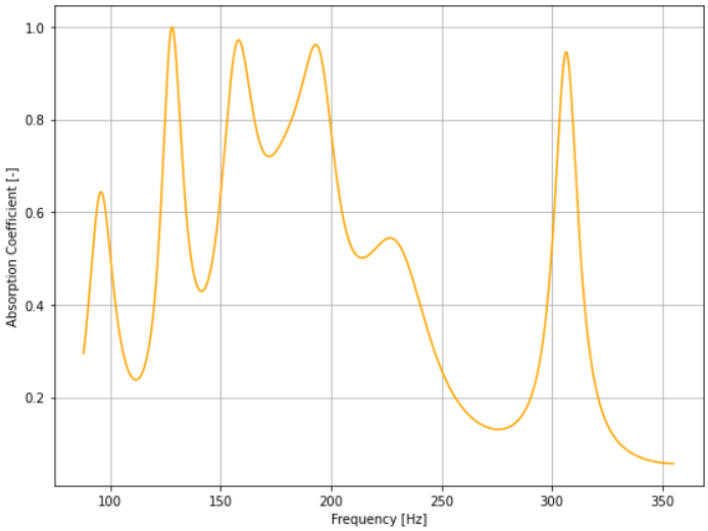

Figure 4.6: The final result of the optimization code, including minimizing of the standard-deviation for the average of averages absorption method

Table 4.6: Tube lengths and diameters for the average of absorption averages with standard-deviation minimizing included

Parameter	**Value**
Length main tube [m]	0.417
Length tube 1 [m]	0.443
Length tube 2 [m]	0.638
Length tube 3 [m]	0.519
Length tube 4 [m]	0.838
Length tube 5 [m]	0.388
Diameter main tube [m]	0.067
Diameter tube 1 [m]	0.011
Diameter tube 2 [m]	0.012
Diameter tube 3 [m]	0.011
Diameter tube 4 [m]	0.021
Diameter tube 5 [m]	0.016
Volume [m^3]	0.002013
Average absorption [-]	0.448

The figure shows a nicely divided absorption spectrum over the whole frequency band. To indicate the difference with only maximization of the absorption over the bandwidth, the volume minimization is temporarily neglected. The result of this adjustment is shown in figure 4.7 and table 4.7.

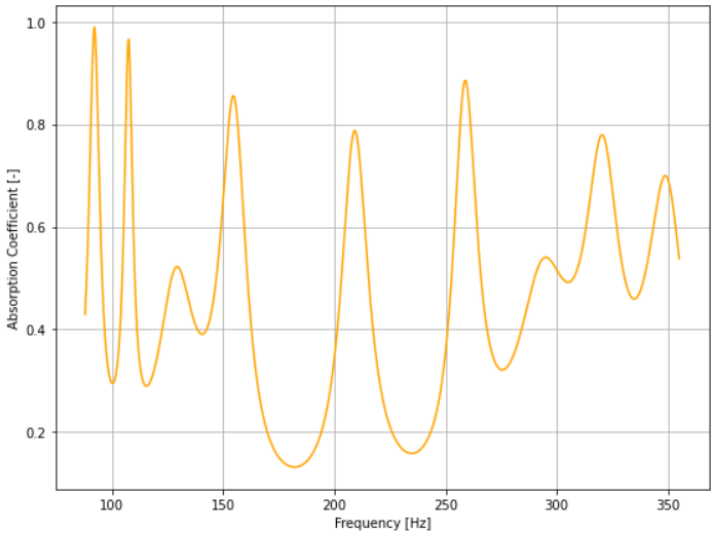

Figure 4.7: Final result of the QWT system optimization, without the minimization of the volume included

Table 4.7: Tube lengths and diameters for the average of absorption averages without minimizing of the volume included

Parameter	Value
Length main tube [m]	0.821
Length tube 1 [m]	0.963
Length tube 2 [m]	0.398
Length tube 3 [m]	0.818
Length tube 4 [m]	0.555
Length tube 5 [m]	0.741
Diameter main tube [m]	0.072
Diameter tube 1 [m]	0.023
Diameter tube 2 [m]	0.021
Diameter tube 3 [m]	0.023
Diameter tube 4 [m]	0.018
Diameter tube 5 [m]	0.025
Volume [m^3]	0.004750
Average absorption [-]	0.454

This result shows an absorption spectrum that is higher than for the case where volume minimization is not neglected, but the volume is much larger. This shows that the optimization indeed minimizes the volume and that this is at the expense of the absorption.

To validate the optimized results, the Pareto front and the convergence plots for the absorption coefficient, the volume and the standard deviation are shown. These are shown in Figure

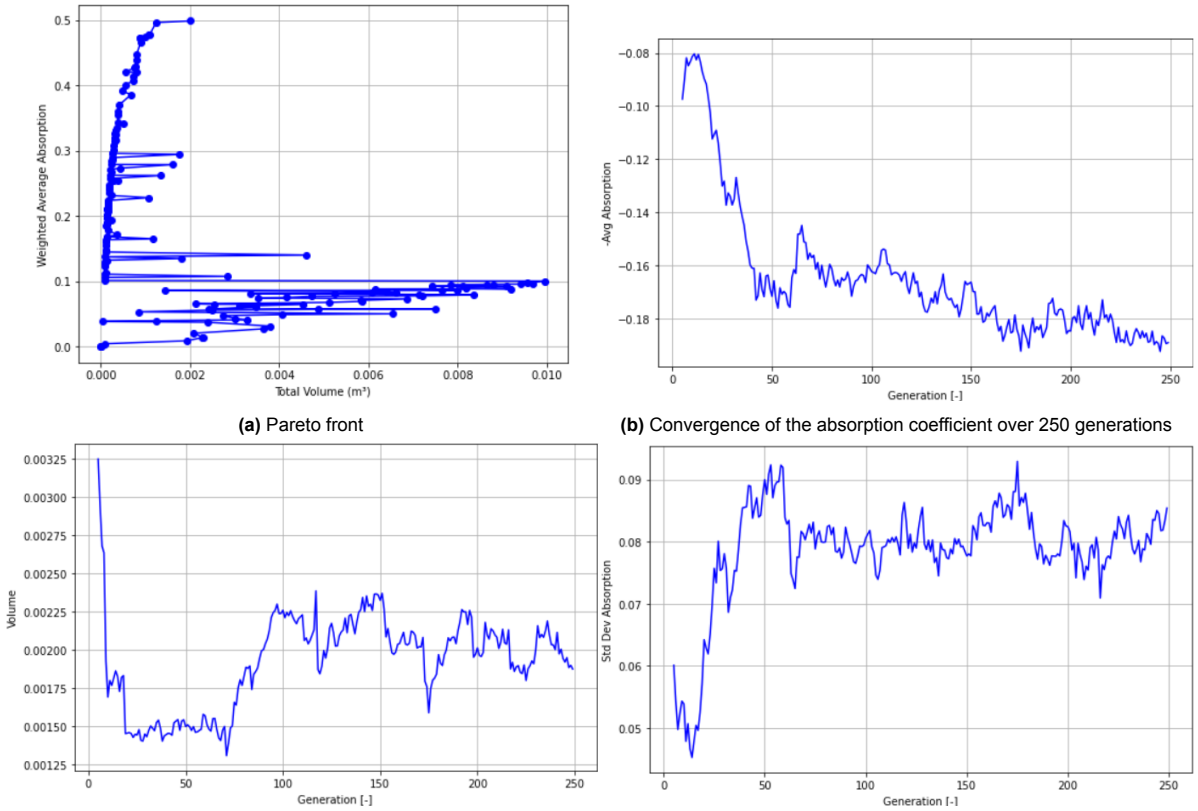

(a) Pareto front

(b) Convergence of the absorption coefficient over 250 generations

(c) Convergence of the volume over 250 generations

(d) Convergence of the standard deviation over 250 generations

Figure 4.8: Pareto front and convergence diagrams of the final optimized QWT system

It should be noted that the average absorption is negative due to the same sign for optimization. These results show that the Pareto front is mostly correct (only many outliers for lower absorption) and the convergence diagrams do actually converge. Therefore, the result of the optimization seems to be plausible.

Another interesting result is to see what the effect of each connected tube is on the final result. To do so, all connected tubes in series are considered individually or none of them at all. This result can be seen in Figures 4.9a up to and including 4.9f.

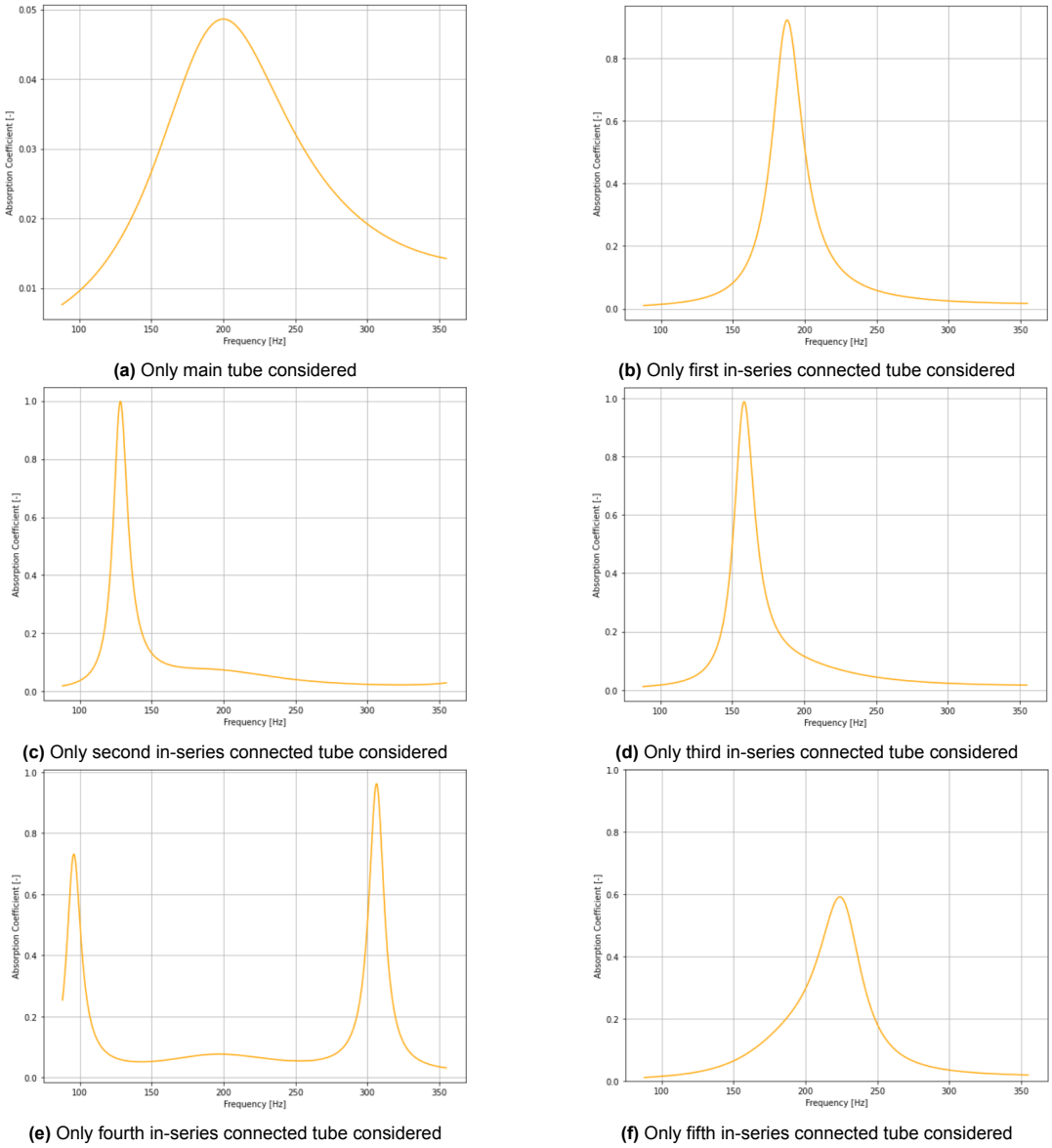

(a) Only main tube considered

(b) Only first in-series connected tube considered

(c) Only second in-series connected tube considered

(d) Only third in-series connected tube considered

(e) Only fourth in-series connected tube considered

(f) Only fifth in-series connected tube considered

Figure 4.9: Effects of individual tubes on final result

It can be clearly seen in all figures what the effect of the in-series connected tubes is: each tube results in a clear peak in the final result. This is an obvious result for tubes that are connected in parallel to each other. However, the height of the absorption peak slightly differs, but this may be due to small porosity changes by removing other tubes. In addition, the effect of the main tube when it is connected in series to one tube is no longer comparable to this situation: the main tube is no longer the central absorbed frequency.

Finally, the porosity of this optimized system is 0.448. This means that on the entire area of the impedance tube with a diameter of 10 cm, 44.8% of the area is occupied by the orifice of the QWT system (35.2 cm^2). In other words, in an area with a diameter of 1 m, namely 7854,0 cm^2, 100 tubes will fit with a total occupied area of 3518.6 cm^2.

Result for further testing

The optimized result obtained has the problem that the main tube with its diameter of 0.067 m. This diameter is very hard to fit in the impedance tube. Therefore, to make it possible to validate the optimization with experimental tests, the volume of the final result is reduced. To do so, only the three higher one-third octave bands are considered, while the diameter cannot be larger than 2 cm. Besides,

the total area of the cross sections of the connected tubes cannot be bigger than 0.5 times the area of the main tube cross section. The result of this reduced volume approach is shown in Figure 4.10 with its corresponding dimensions in 4.8.

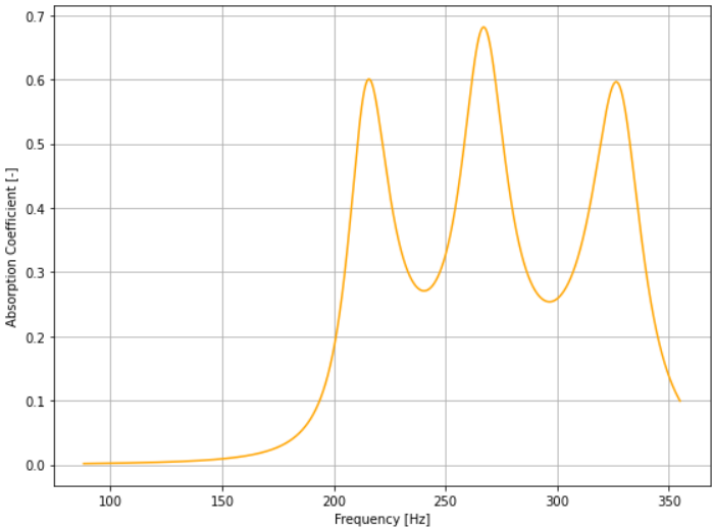

Figure 4.10: Absorption coefficient of QWT system used for further measurements

Table 4.8: Tube lengths and diameters for the QWT system used for further measurements

Parameter	Value
Length main tube [m]	0.303
Length tube 1 [m]	0.269
Length tube 2 [m]	0.0.347
Diameter main tube [m]	0.02
Diameter tube 1 [m]	0.004
Diameter tube 2 [m]	0.004
Volume [m^3]	0.000101

These results are used for the numerical and experimental analyses.

4.2. Numerical results

The numerical analysis is used to bridge the analytical results and the experimental results, as the simulation done with COMSOL gives more accurate results than the Python results, so it can be better compared to the results obtained with the impedance tube. The results are achieved using the Pressure Acoustics physics in combination with Narrow Region Acoustics, and using Pressure Acoustics physics in combination with Thermoviscous Acoustics. The results of these two physics settings in COMSOl are presented in Figure 4.11.

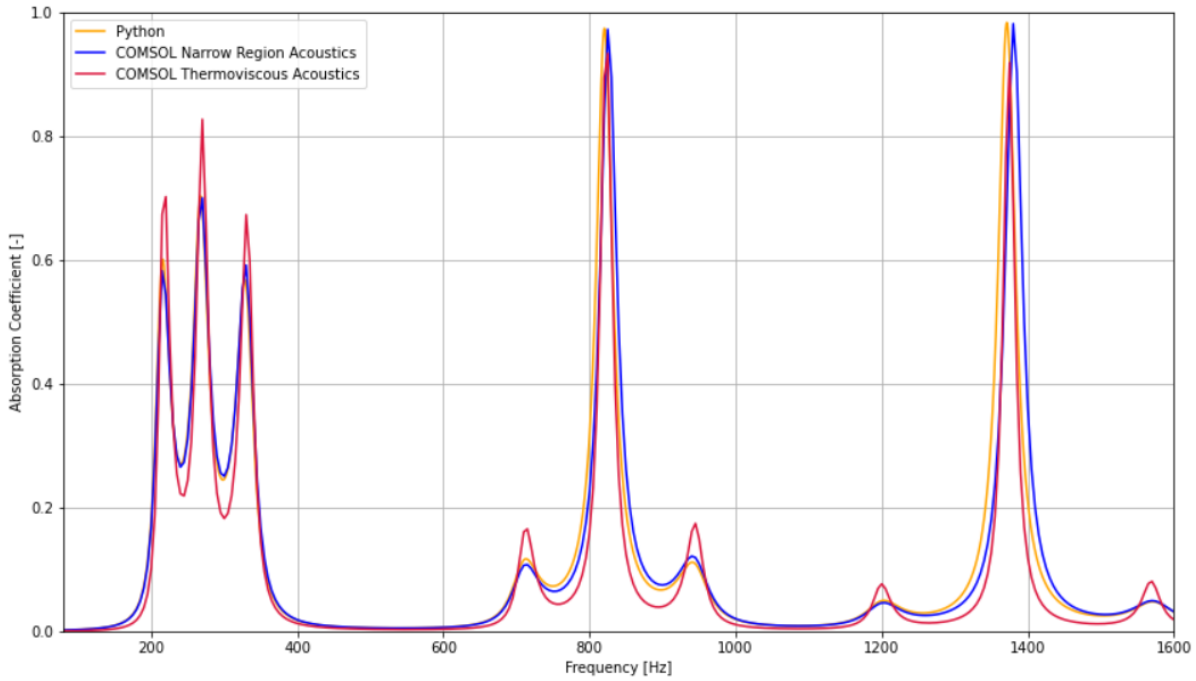

Figure 4.11: Absorption coefficient of QWT system used for further measurements using Python and COMSOL simulations

These results are as expected: the COMSOL result using Narrow Region Acoustics and the Python result align very well. The COMSOL result using Thermoviscous Acoustics do have higher peaks and lower minima. This aligns with the theory that this model better resolves thermoviscous layers in the tubes, so a higher absorption is obtained. These results can be used for the experimental tests using the impedance tube and 3D printed models.

4.3. Experimental results

For the experimental results, the reduced-volume version of the optimized QWT system is 3D printed, and its corresponding absorption coefficients are measured using an impedance tube. Only the reduced version of the optimized QWT system is used, as the optimal solution will not fit the impedance tube because of the large diameter of the main tube. After these measurements, the results of the experimental tests are compared to the Python and COMSOL results. These results are used to answer the following sub-question:

- How do the numerically and analytically received absorption coefficients compare to the experimental results?

First, the printed model is described, followed by the results of the impedance tube measurements.

4.3.1. Final 3D printed model

The 3D printed model used for the final impedance testing is made with the dimensions given in Table 4.8, while using the 3D printer settings given in Appendix C. The printed result is shown in Figure 4.12.

Figure 4.12: The 3D printed model of the reduced volume QWT system for final impedance tube measurements. 150 ml coffee cup for indication of scale. Masking tape applied to ensure casing fits exactly in impedance tube

The model is first put in warm water for 24 hours to dissolve the PVA. However, dissolution of the PVA has shown that a very small hole was present in the model somewhere in the wall of the main tube. More tests are needed to indicate the effect of this hole. The colour change of PLA from black to white has no effect on the absorption of the system.

4.3.2. Results of impedance tube measurements

After calibration of the impedance tube, the model is tested for a frequency bandwidth between 100 and 1600 Hz. The results of these tests are presented in Figure 4.13. As the whole system is optimized for the frequency range between 88 and 355 Hz, the results are zoomed in for this frequency bandwidth in Figure 4.14.

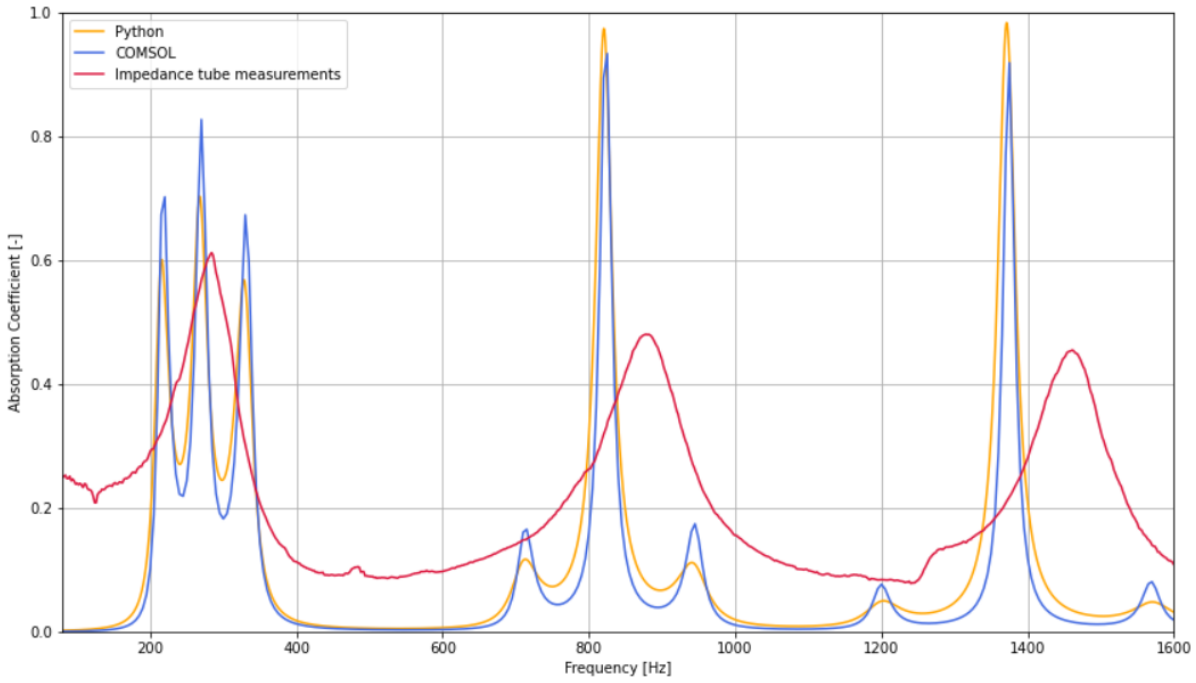

Figure 4.13: Absorption coefficients for Python simulations, COMSOL simulations and impedance tube measurements for the reduced volume QWT system

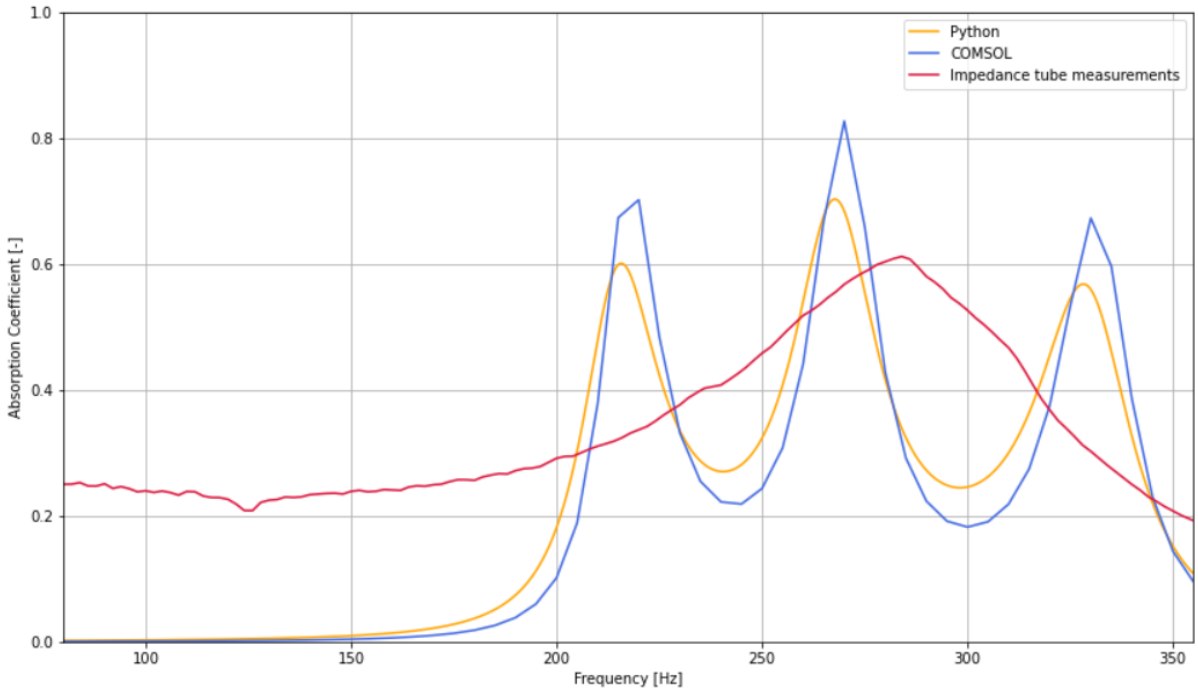

Figure 4.14: Absorption coefficients for Python simulations, COMSOL simulations and impedance tube measurements for the reduced volume QWT system for a smaller bandwidth

Compared to the validation of the printed models (see Section 3.17, the measured results with the impedance tube do not show exactly the to be expected results: an increase of absorption coefficient and a higher resonance frequency by 1-2%. The resonance frequency has indeed shifted to a higher frequency compared to the Python and COMSOL results (with larger shifts for higher frequencies, as can be seen in Figure 4.13, but the absorption peak is in between these results. This could be the first indication that the 3D printed model is not perfect.

For the 3D printed model to fail, a number of possible causes are optional. First, the aforementioned hole has effected the absorption of the whole system. It is possible to prevent this hole from forming, as the hole is possibly caused by removing some PLA treats during aftercare. Secondly, another cause could be that the connected QWTs are not connected completely airtight to the main QWT. The QWTs will not function together as they should be, which will have a huge influence on the absorption spectrum. For example, when the tube with $L = 0.267\ m$ is disconnected from the system, the results will be as shown in Figure 4.15.

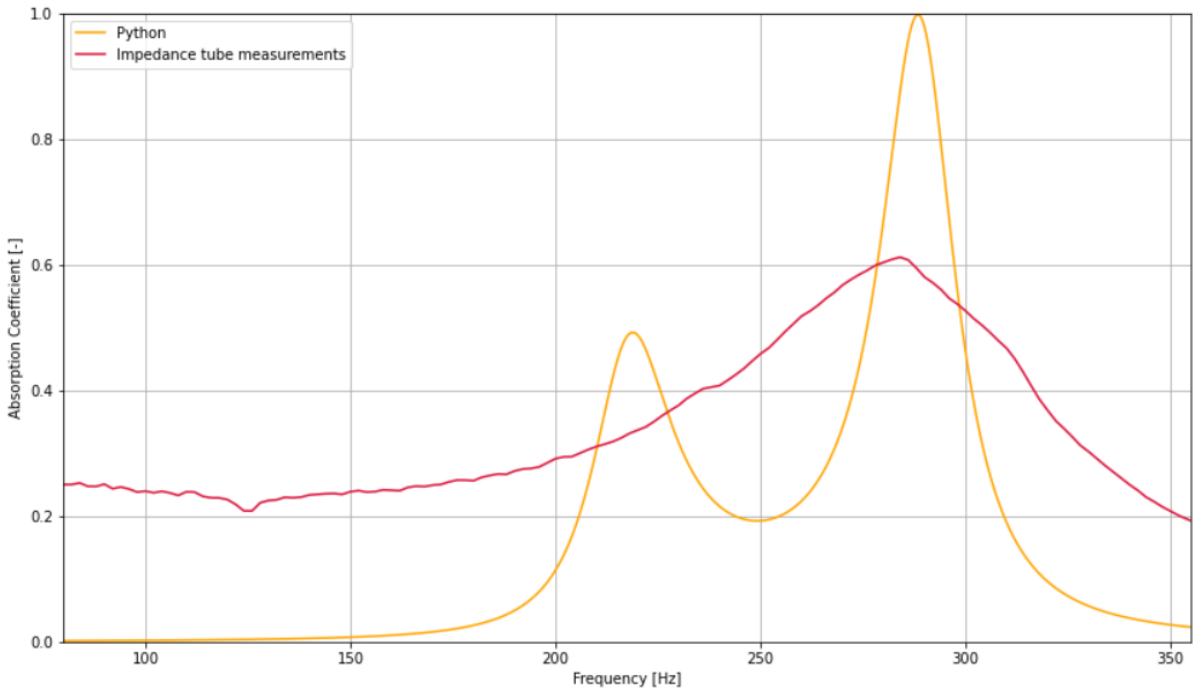

Figure 4.15: Absorption coefficients for Python simulations and impedance tube measurements for the reduced volume QWT system, when the QWT with $L = 0.267\ m$ is removed

This result aligns better with the validation than the previous result in Figure 4.14: the first peak is shifted to a higher frequency, the absorption peak has increased and the other peak has vanished. Therefore, it is possible that the QWT with $L = 0.267\ m$ is not well connected to the main QWT.

The final options for possible misalignment of the results are that the PLA is not completely airtight or that the PVA is not completely dissolved in the tubes. Both options cause a significant negative effect on the absorption of the system. More tests are needed with different wall thicknesses, layer heights, and better tests for total PVA dissolution. For the dissolution of PVA, special removal stations could be used, but were not directly available

5 Discussion

This study explored the development and optimization of a QWT system designed to absorb low-frequency sound efficiently with a minimization of volume of the system excluding tube thicknesses and a maximization of absorption. Analytical modelling, finite element simulations, and experimental tests were used to develop, verify, and validate an optimized system. In this section, the final results are discussed and evaluated. First, the comparison between the three different kinds of analysis is evaluated, followed by an evaluation of the optimization code. Third, the effects of the material used for the 3D printed model are discussed, followed by a discussion about the limitations and neglects in this thesis. Finally, the application of the achieved results is elaborated.

5.1. Comparison of analytical, numerical, and experimental results

The analytical model using the recursive formulation produced an absorption spectrum which aligns quite well with the results of the COMSOL simulations. Pressure Acoustics in combination with Narrow Region Acoustics do align very well, while Pressure Acoustics in combination with Thermoviscous Acoustics result in more accurate result. The Thermoviscous Acoustics simulation captures the thermal and viscous effects inside the QWTs very well.

When 3D printed models were verified and validated, the results align very well with theory: the resonance frequency shifted towards a higher frequency and the absorption peak increased due to bending of the tubes (Cambonie et al., 2018). However, the QWT system consisting of in-series and in-parallel combined tubes did not align as well with the Python and COMSOL results. The absorption spectra did not show the multiple sharp peaks that were present in the analytical and numerical results because the absorption is more spread out for higher frequencies (while the absorption decreases a lot). When the final model was tested, the absorption peak did not increase. Possible reasons for this absence of an increase are 3D printing mistakes, imperfections, or inaccuracies. In addition, a lack of dissolution of the PVA, which is used as the support material, may be the cause of the imperfect result. However, another option is that the Python and COMSOL results are not correct. Although this option is also possible, it is less likely, as the results of other studies that use 3D-printed in-series and/or in-parallel connected systems do align (see, for example, the study of Catapane, Cardone et al. (2023)). More research with more attention to the effects of layer thickness, bending of multiple connected tubes, or wall thicknesses may be needed. In addition, a hole was present in the final model. A good next experiment would be to test a model without holes (except obviously the orifice).

5.2. Results of the optimization code

The optimized QWT system is based on a Python code consisting of DEAP. DEAP, an evolutionary algorithm, depends on many different parameters, such as the number of parents, the number of generations, and the number of offspring. Each parameter has a great influence on the convergence of the result. Although the current values for the parameters are received as converging, more research on the perfect parameter values may be recommended.

Most of the focus in the development of the optimization code was on the determination of ”maximum” absorption over the frequency bandwidth. In this thesis, the maximizing of the absorption is finally done by calculating the average of the average absorption in six different frequency bands. In addition, the standard deviation is minimized. This manner results in a broad absorption spectrum where still a lot of very low minima are present. For next research a further development of the absorption maximization is recommended.

However, the optimization code still gives promising results. When minimization of volume is neglected, the average absorption and especially the volume increases a lot. This is an indication that the optimization code is actually optimizing for minimal volume, but still considers the maximum absorption possible.

5.3. Material of the 3D printed model

For the 3D printed model of the optimized model with reduced volume, PLA is chosen. The choice for PLA is mainly based on its availability at the Faculty of Civil Engineering and Geosciences. Although the results of the verification and validation of the 3D printed models were quite promising, the final measurement was slightly off. 3D printed models with a combination of in-series and in-parallel connected are not much present in research, but the results of 3D printed models of one tube align with the results of other research (see Costa (2016) and Catapane, Petrone et al. (2023)). Other materials, with proven acoustic qualities, are recommended to be used for further tests.

5.4. Effects of limitations and neglects

During the research, several limitations were taken into account to limit the scope. For example, the number of tubes and dimensions of the length and diameter of an QWT were set at fixed values. It may be possible a larger number of tubes causes a very different absorption spectra. The other two variables did not reach their limits during the optimization, so different limits for these variables seem less necessary. Another limit for this thesis was the consideration of just one QWT system. Multiple QWTs will have a huge effect on the porosity. As the volume of the QWT system behind a panel was limited due to the size of the impedance tube, no more number of equal QWT systems could be considered. One of the main recommendations for next research would be to include this consideration.

Other limitations were not chosen, but obligated. For example, the QWT system had to fit the impedance tube. The fixed size results in a fixed area for porosity calculations and limitations for the size of the QWT system. The next step for proving the absorption qualities of the QWT system would be to do free field measurements.

5.5. Application in engineering context

As this research is positioned within the field of civil engineering, the application potential of the optimized QWT system is a crucial consideration. The findings are particularly relevant for the design of building enclosure, acoustic panels, and interior walls where low frequency noise mitigation is needed but space is limited.

To determine how much surface area of panels consisting of these systems is needed, Sabine’s equation 2.4 could be used. If the actual and desired reverberation times are known for the frequency bands of interest (besides the volume and surface area of the room), the area of the panels can be calculated. This is done by calculating the difference in area between the two situations (desired and actual reverberation time) and dividing this difference by the average absorption coefficient over the (one-third) octave band. This calculation should be done over the different (one-third) octave bands in the frequency band of interest, and the largest calculated absorption area is normative. It should be noted that this calculation is only applicable in closed rooms. An impression how such panels would fit in a room can be seen in Figure 5.1.

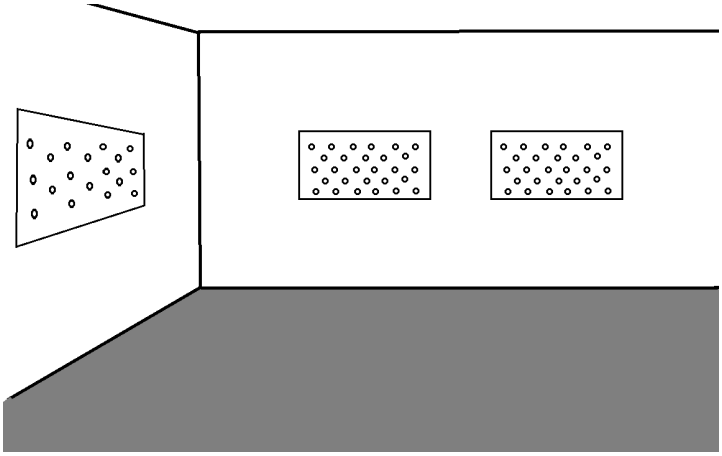

Figure 5.1: A schematic impression how panels consisting of quarter-wavelength tube systems would fit in a room

There are different types of applications where QWT systems can be useful. Potential real-life applications include:

- HVAC and mechanical plant rooms: Where equipment generates consistent low frequency noise, the compact absorber panels developed here could be integrated into walls or ceilings.
- Architectural acoustics in public spaces: Concert halls, theatres, recording studios, or auditoriums often require targeted control of low frequency reverberation without compromising aesthetics or space usage. The coiled and optimized design of the QWT systems offers customizable integration in acoustic panels for such rooms.
- Residential buildings and offices: In urban environments, low frequency noise from traffic or adjacent machinery can be a significant disturbance. These QWT systems, embedded in facades or ceilings, could offer as a solution.
- Lightweight structures: In timber or other lightweight made buildings where traditional mass-based soundproofing is not feasible, QWT systems provide a volume-efficient and material-efficient way to improve acoustic performance without significantly adding weight or thickness.

From a structural engineering standpoint, the optimized QWT system allows integration into panel-based systems, with potential to standardize elements for modular construction. Moreover, the fact that these systems can be 3D printed could make it very accessible to make such panels. Therefore, in contrast to some standard absorption materials mentioned in Chapter 2.1.3, optimized QWT systems do have added value. Especially when a specific broad absorption spectrum needs to be absorbed, the proposed system could be useful. The proposed QWT system has as main advantages that it uses less volume than most standard absorbers (when correctly designed) or they have the ability to absorb much lower frequencies and a broader bandwidth, or both. However, large scale production of such systems would be quite expensive compared to similar absorbers. Besides, 3D printing is very time consuming, which is detrimental for the manufacturability of QWT systems. Therefore, the proposed system is most advisable when the absorption of a specific low-frequency bandwidth is essential and alternative solutions prove inadequate, making the associated costs and production drawbacks justifiable.

It should be noted, however, that 3D printed QWT systems consisting of a combination of in-series and in-parallel connected tube should be tested in more detail, as the results do not align with the Python and COMSOl results at this moment.

6

Conclusion

The goal of this thesis was to answer the following research question: *What is the optimal configuration using minimal volume of a main quarter-wavelength tube connected in series with multiple parallel tubes for the absorption of frequencies between 88 and 355 Hz?*. To achieve the answer of this question, a Python code is written to optimize the quarter-wavelength system for maximal absorption and minimal volume. Afterwards, the proposed system is simulated using COMSOL to achieve more accurate results. For the impedance tube measurements, the proposed system is 3D printed and made of PLA.

To understand the quarter-wavelength system made of a combination of in-parallel and in-series connected tubes, the influence of the diameter of each tube, length of each tube and number of connected tubes are researched. The most important aspect of each tube turned out to be its length, as the length determines the resonance frequency of the tube. The diameter causes mostly viscothermal effects which also causes absorption. When tubes are placed in parallel, the tubes act independently. This means that more tubes increase the absorption spectrum. However, in-series connection of the tubes influences the absorption of the system significantly.

The optimization code which uses DEAP, an evolutionary algorithm, results in a configuration of one main tube connected to five smaller tubes. The optimization is done by maximizing the absorption by taking the average of the absorption average in six different frequency bands. Including minimization of volume causes the volume (excluding tube wall thicknesses) to decrease with 2731 cm^3, while the absorption stays approximately the same (0.417 for minimization of the volume, 0.454 without the minimization). However, the optimized system is still too large to fit in the impedance tube, which is used for the experimental analysis. Therefore, a quarter-wavelength tube system with reduced volume is chosen. This reduced volume system contains just two connected tubes instead of five.

The COMSOL simulations, done with Pressure Acoustics in combination with Narrow Region Acoustics and Pressure Acoustics in combination with Thermoviscous Acoustics, align very well with the simulations. The Narrow Region Acoustics uses the same model as the Python code (low reduced frequency), which results in almost exactly the same results. Thermoviscous Acoustics uses a linearized Navier-Stokes model, which is more exact than Narrow Region Acoustics. The absorption peaks are higher for Thermoviscous Acoustics, but still align with the Python absorption spectrum. As the Thermoviscous Acoustics model was more accurate, this one was used for comparison with the experimental results.

The reduced volume optimized quarter-wavelength tube system was 3D printed using an Ultimaker S5 and tested with an impedance tube. This model was coiled, in contrast to other digital models. The effect of coiling is a shift of the resonance frequency towards higher frequencies and an increase of the absorption peaks. However, the actual 3D printed model shows a different absorption result than the Python and COMSOL results, as the absorption peak does not really increase and the form of the absorption spectra does not align. Possible causes for this result are a hole present in the 3D printed model, a poor connection between the different tubes, too little dissolution of the support material, or lack of airtightness of the walls. The most likely causes are the presence of a hole and too little

dissolution of the support material. The experimental results are likely unreliable, since in other studies they align with numerical results. The analytical and numerical results are therefore more trusted.

In conclusion, the proposed optimization of the quarter-wavelength configuration consisting of in-parallel and in-series connected tubes for the absorption of low frequency sound show promising results. The optimized system consisting of one main tube connected in series with five parallel tubes show a clear decrease of volume compared to a system of tubes without minimizing the volume. The proposed system aligns very well with finite element simulations, but real-life tests do not yet confirm that the system will function the same in real life. The most likely causes are that the airtightness is not guaranteed due to the presence of a hole in the wall of a tube or too little dissolution of the support material. However, results are very promising, but more accurate impedance tube measurements are needed.

7

Recommendations

Not all aspects of optimized quarter-wavelength tube systems for low frequencies could be handled during this thesis. Some parts include some limitations that could be neglected in other studies, while other parts are not done due to time/scope limitations. The analytical and experimental parts have the most potential for further research, as these parts include the most limitations, room for further research, and options to do the same research in a different way. Therefore, some recommendations are given in this chapter for further research.

Recommendations for the analytical analysis

The analytical analysis consists of Python code including the recursive formulation and DEAP for optimization. However, much room is left for further research. Some aspects that could be researched are:

- Number of tubes: for this study, only one tube system is considered over the cross section of an impedance tube. It is recommended to investigate the effect of more of the same tube systems per cross section of an impedance tube, different kinds of systems per cross section, or both. This way, it may be possible to have higher absorption over the frequency band
- Porous absorbers: it is possible to place porous absorbers at the orifice of a QWT system (Setaki et al., 2016). The effect of such absorbers is positive for the total absorption, but this is neglected for this research. It is recommended to test the influence of such absorbers for this system.
- Limitations of DEAP: for DEAP, the dimensions (lengths, diameters, number of connected tubes) are limited. The effect of different values is recommended to fully cover the effect of the optimization code.
- Comparison of code: The final code using recursive formulation and DEAP is only compared with Van der Eerden (2000) for the recursive formulation part. More comparisons could be useful to fully verify the code. Besides, the DEAP part is for now not compared with any other study. To fully trust the result of DEAP, the results should be compared with comparable studies.

Recommendations for the experimental analysis

The experimental analysis mostly include recommendations for topics that are not done in this study due to limitations of time, material, or both. Some of these recommendations include:

- Removal of PVA: The final results of the experimental analysis are not as expected. A possible reason for this is that the PVA in the 3D printed model is not completely dissolved. Better manners for PVA dissolution should be investigated to confirm (or deny) this hypothesis.
- The use of PLA: for the physical model, only PLA is used. Other kinds of material should also be considered, and ideally a material where the possibility of incomplete airtightness is near zero. Another considered option for the experimental results is the occurrence of a hole in the printed model, so a material where this could be neglected or where the holes could be easier closed is advised.

- Limitations of impedance tube: the effect of the QWT system is only investigated in an impedance tube. A panel consisting of multiple QWT systems in a room will result in additional information about the effect of QWT systems on sound absorption.
- Rhino model of QWT system: the Rhino model for the 3D printing is not yet optimal, as the model is still not very thin. This could be improved in the future.

Other recommendations could be the application of the system to other frequency bands and/or the optimization of other kinds of QWT systems, such as multiple in-series connected QWTs.

References

Beltman, W. (1999). Viscothermal wave propagation including acousto-elastic interaction, part ii: Applications. *Journal of Sound and Vibration*, *227*(3), 587–609. https://doi.org/10.1006/jsvi.1999.2356

Bergh, H., & Tijdeman, H. (1965). Theoretical and experimental results for the dynamic response of pressure measuring systems.

Berglund, B., Hassmén, P., & Job, R. F. S. (1996). Sources and effects of low-frequency noise. *The Journal of the Acoustical Society of America*, *99*(5), 2985–3002. https://doi.org/10.1121/1.414863

Bezemer-Krijnen, M. (2018). *Sound absorption of porous structures: A design tool for road surfaces* [Doctoral dissertation, University Library/University of Twente]. https://doi.org/10.3990/1.9789036545846

Cai, X., Guo, Q., Hu, G., & Yang, J. (2014). Ultrathin low-frequency sound absorbing panels based on coplanar spiral tubes or coplanar helmholtz resonators. *Applied Physics Letters*, *105*(12). https://doi.org/10.1063/1.4895617

Cambonie, T., Mbailassem, F., & Gourdon, E. (2018). Bending a quarter wavelength resonator : Curvature effects on sound absorption properties. *Applied Acoustics*, *131*, 87–102. https://doi.org/10.1016/j.apacoust.2017.10.004

Carvalho de Sousa, A., Deckers, E., Claeys, C., & Desmet, W. (2021). On the assembly of archimedean spiral cavities for sound absorption applications: Design, optimization and experimental validation. *Mechanical Systems and Signal Processing*, *147*, 107102. https://doi.org/10.1016/j.ymssp.2020.107102

Catapane, G., Cardone, L. M., Petrone, G., Robin, O., & Franco, F. (2023). Coupling effect of acoustic resonators for low-frequency sound suppression. *Aeronautics and Astronautics - AIDAA XXVII International Congress*, *37*, 254–257. https://doi.org/10.21741/9781644902813-55

Catapane, G., Petrone, G., Robin, O., & Verdière, K. (2023). Coiled quarter wavelength resonators for low-frequency sound absorption under plane wave and diffuse acoustic field excitations. *Applied Acoustics*, *209*, 109402. https://doi.org/10.1016/j.apacoust.2023.109402

COMSOL Multiphysics. (2018). *Acoustics module user's guide* [Version 5.4]. COMSOL AB. https://doc.comsol.com/5.4/doc/com.comsol.help.aco/AcousticsModuleUsersGuide.pdf

Costa, S. (2016). *Thin low-frequency sound absorbing panel by additive manufacturing* [Master Thesis]. Faculty of Architecture, Department of Building Technology.

Cox, T. J., & D'Antonio, P. (2016). *Acoustic absorbers and diffusers: Theory, design and application* (3rd). CRC Press.

De Bie, F., Denayer, H., Claeys, C., & Deckers, E. (2022). Quarter-wavelength acoustic metamaterials: The effect of folding on the resonance frequency. *Proceedings of ISMA2022-USD2022*.

Deb, K., Pratap, A., Agarwal, S., & Meyarivan, T. (2002). A fast and elitist multiobjective genetic algorithm: Nsga-ii. *IEEE Transactions on Evolutionary Computation*, *6*(2), 182–197. https://doi.org/10.1109/4235.996017

Field, C., & Fricke, F. (1998). Theory and applications of quarter-wave resonators: A prelude to their use for attenuating noise entering buildings through ventilation openings. *Applied Acoustics*, *53*(1–3), 117–132. https://doi.org/10.1016/s0003-682x(97)00035-2

Ford, R., & McCormick, M. (1969). Panel sound absorbers. *Journal of Sound and Vibration*, *10*(3), 411–423. https://doi.org/10.1016/0022-460x(69)90219-3

Gommer, B. (2016, October). *Resistance in helmholtz resonators: Exploring the potential of sound absorption created by additive manufacturing* [Master's thesis]. Delft University of Technology. https://repository.tudelft.nl/record/uuid:68402550-3641-46ce-b3b2-3b43c4fe9442

Hunecke, J. (2024). Panel absorbers [Accessed: 2025-05-22]. https://www.hunecke.de/en/knowledge/absorbers/panel-absorbers.html

International Organization for Standardization. (2023). NEN-EN-ISO 10534-2:2023 - acoustics — determination of sound absorption coefficient and impedance in impedance tubes — part 2: Transfer-function method [Dutch version: NEN-EN-ISO 10534-2:2023].

Kafle, A., Luis, E., Silwal, R., Pan, H. M., Shrestha, P. L., & Bastola, A. K. (2021). 3d/4d printing of polymers: Fused deposition modelling (fdm), selective laser sintering (sls), and stereolithography (sla). *Polymers*, *13*(18), 3101. https://doi.org/10.3390/polym13183101

Kuczmarski, M. A., & Johnston, J. C. (2011). *Acoustic absorption in porous materials* (NASA Technical Memorandum No. NASA/TM-2011-216995) (NASA Technical Report, Document ID: 20110011143). NASA Glenn Research Center. https://ntrs.nasa.gov/citations/20110011143

Maa, D.-Y. (1975). Theory and design of microperforated panel sound-absorbing constructions. *Scientia Sinica*, *18*(1), 55–71. https://doi.org/10.1360/YA1975-18-1-55

Ng, N., Abdul Haq, R., Marwah, O., Ho, F., & Adzila, S. (2022). Optimization of polyvinyl alcohol (pva) support parameters for fused deposition modelling (fdm) by using design of experiments (doe). *Materials Today: Proceedings*, *57*, 1226–1234. https://doi.org/10.1016/j.matpr.2021.11.046

Pang, X., Zhuang, X., Tang, Z., & Chen, X. (2010). Polylactic acid (pla): Research, development and industrialization. *Biotechnology Journal*, *5*(11), 1125–1136. https://doi.org/10.1002/biot.201000135

Parker, N. G., Mather, M. L., Morgan, S. P., & Povey, M. J. W. (2010). Longitudinal acoustic properties of poly(lactic acid) and poly(lactic- co -glycolic acid). *Biomedical Materials*, *5*(5), 055004. https://doi.org/10.1088/1748-6041/5/5/055004

Qiu, X. (2016). Principles of sound absorbers. In *Acoustic textiles* (pp. 43–72). Springer Singapore. https://doi.org/10.1007/978-981-10-1476-5_3

Rayleigh, J. W. S. (1945). *The theory of sound* (Vol. 2). Dover Publications, New York.

Salter, C. M. (1998). *Acoustics: Architecture, engineering, the environment*. William Stout Publishers.

Scholten, T. (2018). *Broadband absorption using coupled quarter wavelength tubes* [Master's thesis]. Delft University of Technology. https://repository.tudelft.nl/record/uuid:d5528ff7-a509-4ddb-aff8-aa1f847a0056

Setaki, F., Tenpierik, M., Timmeren, A., & Turrin, M. (2016). New sound absorption materials: Using additive manufacturing for compact size, broadband sound absorption at low frequencies. *INTER-NOISE 2016*.

Tijdeman, H. (1975). On the propagation of sound waves in cylindrical tubes. *Journal of Sound and Vibration*, *39*(1), 1–33. https://doi.org/10.1016/s0022-460x(75)80206-9

Van der Eerden, F. (2000, November). *Noise reduction with coupled prismatic tubes* [PhD Thesis - Research UT, graduation UT]. University of Twente. University of Twente.

Waye, K. (2011). Effects of low frequency noise and vibrations: Environmental and occupational perspectives. In *Encyclopedia of environmental health* (pp. 240–253). Elsevier. https://doi.org/10.1016/b978-0-444-52272-6.00245-2

Zwikker, C., & Kosten, C. (1949). *Sound absorbing materials*. Elsevier Publishing Company. https://books.google.nl/books?id=AkghAAAAMAAJ

A

Python code for the coupled tubes system

```python
import numpy as np
import matplotlib.pyplot as plt
from scipy.special import jn
import pandas as pd
from itertools import islice
from deap import base, creator, tools, algorithms
import random

class CoupledTubes:
    def __init__(self, frequency, tube_lengths, tube_diameters, porosity, gamma=1.4, rho0=1.22, c0=343.3, mu=18.2e-6, cp=1005):
        """
        Initialize the coupled tubes system.

        Parameters:
        - frequency: Array of frequencies (Hz) for analysis.
        - tube_lengths: List of lengths of the tubes (m).
        - tube_diameters: List of diameters of the tubes (m).
        - Porosity: porosity of the material (-). For now it is an parameter, but the calculation for the porosity could be included in the future.
        - gamma: Adiabatic constant for air (default: 1.4).
        - rho0: Air density (kg/m³) (default: 1.22).
        - c0: Speed of sound in air (m/s) (default: 343.3).
        - mu: Dynamic viscosity of air (Pa·s) (default: 18.2e-6).
        - cp: Specific heat capacity of air (J/kg·K) (default: 1005).
        """
        self.frequency = np.array(frequency) # Frequencies to analyze
        self.omega = 2 * np.pi * self.frequency # Angular frequencies
        self.wave_length = 343 / self.frequency # Wavelength
        self.tube_lengths = np.array(tube_lengths) # Tube lengths
        self.tube_diameters = np.array(tube_diameters) # Tube diameters
        self.porosity = porosity # Porosity of the material
        self.tube_radii = self.tube_diameters / 2 # Tube radii
        self.tube_lengths[0] += (8*self.tube_radii[0])/(3*np.pi) # Tube lengths with end corrections included
        self.tube_lengths[1:] += ((8*self.tube_radii[1:])/(3*np.pi)) * (1 - 1.25 * (self.tube_radii[1:] / self.tube_radii[0])) # Tube lengths with end corrections included
        self.gamma = gamma # Adiabatic constant for air
        self.rho0 = rho0 # Air density
        self.c0 = c0 # Speed of sound in air
        self.Z0 = self.rho0 * self.c0  # Characteristic impedance of air
        self.mu = mu # Dynamic viscosity of air
        self.cp = cp # Specific heat capacity of air

    def shear_wave_number(self, radius):
```

```
        #shape = frequencies
        """
        Calculate the shear wave number s.
        """
        return radius * np.sqrt(self.omega * self.rho0 / self.mu)

    def squared_prandtl_number(self):
        """
        Calculate the squared Prandtl number sigma.
        """
        return  0.84 #np.sqrt((self.mu * self.cp)/self.wave_length) (squared prandtl number
            is a constant for air)

    def propagation_coefficient(self, shear_wave):
        """
        Compute the propagation coefficient Gamma using the Low Reduced Frequency Model.
        """
        n = (1+(self.gamma-1)/self.gamma * (jn(2, 1j*np.sqrt(1j)*self.squared_prandtl_number
            ()*shear_wave))/jn(0, 1j*np.sqrt(1j)*self.squared_prandtl_number()*shear_wave))
            **-1
        return np.sqrt((jn(0, 1j*np.sqrt(1j)*shear_wave)*self.gamma)/(jn(2, 1j*np.sqrt(1j)*
            shear_wave)*n))

    def calculate_G(self, propagation_coefficient, shear_wave):
        """
        Calculate the factor G for the viscothermal effects.
        """
        n = (1+(self.gamma-1)/self.gamma * (jn(2, 1j*np.sqrt(1j)*self.squared_prandtl_number
            ()*shear_wave))/jn(0, 1j*np.sqrt(1j)*self.squared_prandtl_number()*shear_wave))
            **-1
        return - (1j / propagation_coefficient) * (self.gamma/n)

    def transfer_function_parallel(self, length, radius, shear_wave):
        """
        Compute the transfer function for the parallel tubes connected in series with another
             main tube.
        Includes viscothermal effects via Gamma and G.
        """

        Gamma = self.propagation_coefficient(shear_wave)
        G = self.calculate_G(Gamma, shear_wave)

        # Wave number in the tube
        k = self.omega / self.c0
        area = np.pi * radius**2

        # Compute sinh and cosh terms
        sinh_term = np.sinh(Gamma * k * length)
        cosh_term = np.cosh(Gamma * k * length)
        return (area*G/sinh_term)*(cosh_term-cosh_term**-1)

    def transfer_function_main(self, length, radius, shear_wave, transfer_parallel_total):
        """
        Compute the transfer function for the main tube.
        Includes viscothermal effects via Gamma and G.
        """
        Gamma = self.propagation_coefficient(shear_wave)
        G = self.calculate_G(Gamma, shear_wave)
        # Wave number in the tube
        k = self.omega / self.c0
        area = np.pi * radius**2
        # Compute sinh and cosh terms
        sinh_term = np.sinh(Gamma * k * length)
        cosh_term = np.cosh(Gamma * k * length)
        transfer_function_main = (cosh_term + sinh_term/(area*G)*transfer_parallel_total)**-1
        return cosh_term, sinh_term, transfer_function_main

    def impedance_at_begin(self):
        """
        Calculate the acoustic impedance at the beginning of the tube-system.
        """
```

```
        # Parallel tubes
        transfer_parallel_total = 0
        for length, radius in zip(self.tube_lengths[1:], self.tube_radii[1:]):
            shear_wave = self.shear_wave_number(radius)
            transfer_parallel_total += self.transfer_function_parallel(length, radius,
                shear_wave)
        # Main tube
        main_length = self.tube_lengths[0]
        main_radius = self.tube_radii[0]
        shear_wave = self.shear_wave_number(main_radius)
        Gamma = self.propagation_coefficient(shear_wave)
        G = self.calculate_G(Gamma, shear_wave)
        cosh_term, sinh_term, transfer_function_main = self.transfer_function_main(
            main_length, main_radius, shear_wave, transfer_parallel_total
        )

        # Compute scaled impedance
        scaled_impedance = sinh_term / (cosh_term - transfer_function_main)
        # Compute impedance
        impedance = (self.Z0/-G) * scaled_impedance
        return impedance, scaled_impedance

    def absorption_coefficient(self):
        """
        Calculate the absorption coefficient of the material.
        """
        impedance_za, impedance_dzeta = self.impedance_at_begin()
        impedance = 1 / (self.porosity / impedance_za) # Include porosity effects
        impedance_scaled = 1 / (self.porosity / impedance_dzeta)
        reflection_coefficient = (impedance - self.Z0) / (impedance + self.Z0)
        absorption = 1 - np.abs(reflection_coefficient) ** 2
        return absorption, impedance_scaled


    def compute(self):
        """
        Compute the acoustic response at all frequencies.
        """
        absorption, impedance_scaled = self.absorption_coefficient()
        return {
            "frequency": self.frequency,
            "impedance_magnitude": np.abs(impedance_scaled),
            "impedance_phase": np.angle(impedance_tube),
            "absorption_coefficient": absorption,
        }
```

B

Python code for the optimization

```python
import numpy as np
import matplotlib.pyplot as plt
from scipy.special import jn
import pandas as pd
from itertools import islice
from deap import base, creator, tools, algorithms
import random

# Set random seeds for reproducibility
np.random.seed(42)
random.seed(42)

# Define the fitness function
def evaluate(individual):
    # Get number of connected tubes
    num_connected_tubes = int(round(individual[12]))  # The 13th value represents the number of connected tubes
    num_connected_tubes = max(2, min(num_connected_tubes, 5))  # Ensure it's within valid range
    individual[12] = num_connected_tubes  # Store the corrected value

    # Enforce constraints (repair invalid individuals)
    for i in range(12):  # Lengths and Diameters
        if i < 6:
            individual[i] = max(0.01, min(individual[i], 1.0))  # Lengths between 10mm and 2 meters
        else:
            individual[i] = max(0.001, min(individual[i], 0.1))  # Diameters between 0.001 and 0.2 meters

    lengths = individual[:6]
    diameters = individual[6:12]

    # Ensure total cross-sectional area of connected tubes is less than or equal to the main tube area
    total_connected_area = sum(np.pi * (d / 2)**2 for d in diameters[1:num_connected_tubes+1])
    main_tube_area = np.pi * (diameters[0] / 2)**2
    if total_connected_area > 0.8 * main_tube_area:
        return 1e6, 1e6, 1e6  # Penalize invalid solutions

    # Porosity calculation remains unchanged
    porosity = (np.pi * (diameters[0] / 2)**2) / 0.0079  # Calculate porosity

    # Penalize invalid porosity values
    if porosity <= 0 or porosity > 1:
        return 1e6, 1e6, 1e6  # Penalize invalid solutions

    # Ensure lists are not empty before passing to CoupledTubes
```

```
    tube_lengths = lengths[:num_connected_tubes+1]
    tube_diameters = diameters[:num_connected_tubes+1]

    # Create the coupled tube system
    tubes = CoupledTubes(
        frequency=np.linspace(88, 355, 1000),
        tube_lengths=tube_lengths,
        tube_diameters=tube_diameters,
        porosity=porosity
    )

    # Compute the absorption coefficient
    result = tubes.compute()
    absorption = result["absorption_coefficient"]

    # Ensure the absorption is valid
    if np.any(absorption < 0) or np.any(np.isnan(absorption)):
        return 1e6, 1e6, 1e6  # Penalize invalid solutions

    # Compute weighted average absorption coefficient for different frequency ranges
    freq = tubes.frequency
    avg_1 = np.mean(absorption[(freq >= 89.1) & (freq <= 112)])
    avg_2 = np.mean(absorption[(freq > 112) & (freq <= 141)])
    avg_3 = np.mean(absorption[(freq > 141) & (freq <= 178)])
    avg_4 = np.mean(absorption[(freq > 178) & (freq <= 224)])
    avg_5 = np.mean(absorption[(freq > 224) & (freq <= 282)])
    avg_6 = np.mean(absorption[(freq > 282) & (freq <= 355)])

    weighted_avg = (avg_1 + avg_2 + avg_3 +
                    avg_4 + avg_5 + avg_6)/6  # Prioritize middle bands

    # Compute standard deviation of the absorption averages
    std_dev = np.std([avg_1, avg_2, avg_3, avg_4, avg_5, avg_6])
    volumes = [np.pi * (d / 2)**2 * l for d, l in zip(tube_diameters, tube_lengths)]
    total_volume = sum(volumes)

    penalty = 1e3 * abs(min(0, porosity)) + 1e3 * abs(max(0, porosity - 1))
    # Return the fitness values, maximize weighted average, minimize volume, and minimize
        standard deviation
    return -weighted_avg, total_volume + penalty, std_dev

# Problem setup
creator.create("FitnessMin", base.Fitness, weights=(-1.0, -1.0, -1.0))  # Minimize weighted
    average, volume, and std deviation
creator.create("Individual", list, fitness=creator.FitnessMin)
toolbox = base.Toolbox()

# Attribute generation with bounds
toolbox.register("attr_length", np.random.uniform, 0.01, 1.0)  # Tube lengths (between 1 mm
    and 2 meters)
toolbox.register("attr_diameter", np.random.uniform, 0.001, 0.1)  # Tube diameters (between
    0.001 and 0.2 meters)
toolbox.register("attr_connected_tubes", np.random.randint, 2, 6)  # Number of connected
    tubes (between 2 and 5)

# Individual and population
toolbox.register("individual", tools.initCycle, creator.Individual,
                 (toolbox.attr_length,) * 6 + (toolbox.attr_diameter,) * 6 + (toolbox.
                     attr_connected_tubes,), n=1)
toolbox.register("population", tools.initRepeat, list, toolbox.individual)

# Operators
toolbox.register("evaluate", evaluate)
toolbox.register("mate", tools.cxBlend, alpha=0.5)
toolbox.register("mutate", tools.mutGaussian, mu=0, sigma=0.1, indpb=0.2)

def mutUniform(individual, low, up, indpb):
    for i in range(len(individual)):
        if random.random() < indpb:
            individual[i] = random.uniform(low[i], up[i])
    return individual,
```

```
109
110 bounds_low = [0.01] * 6 + [0.001] * 6 + [2]  # Bounds for lengths, diameters, and connected
        tubes
111 bounds_up = [1.0] * 6 + [0.1] * 6 + [5]
112 toolbox.register("mutate", mutUniform, low=bounds_low, up=bounds_up, indpb=0.2)
113
114 def cxBounded(ind1, ind2):
115     tools.cxBlend(ind1, ind2, alpha=0.5)
116     return ind1, ind2
117
118 toolbox.register("mate", cxBounded)
119 toolbox.register("select", tools.selNSGA2)
120
121 # Run the optimization
122 population = toolbox.population(n=150)
123 algorithms.eaMuPlusLambda(population, toolbox, mu=150, lambda_=150, cxpb=0.9, mutpb=0.1, ngen
        =200,
124                           stats=None, halloffame=None, verbose=True)
```

C

Additive manufacturing settings in Ultimaker Cura

Setting	Extruder 1	Extruder 2
Layer Height	0.15 mm	0.15 mm
Wall Thickness	0.8 mm	0.8 mm
Wall Line Count	2	2
Horizontal Expansion	-0.015 mm	-0.015 mm
Top/Bottom Thickness	1.0 mm	1.0 mm
Top Thickness	1.0 mm	1.0 mm
Top Layers	7	7
Bottom Thickness	1.0 mm	1.0 mm
Bottom Layers	7	7
Infill Density	100.0%	100.0%
Infill Pattern	Grid	Grid
Printing Temperature	205.0 °C	220.0 °C
Build Plate Temperature	60 °C	60 °C
Print Speed	50.0 mm/s	20.0 mm/s
Enable Retraction	Yes	Yes
Retraction Distance	6.5 mm	6.5 mm
Retraction Speed	25.0 mm/s	45.0 mm/s
Z Hop When Retracted	Yes	Yes
Enable Print Cooling	Yes	Yes
Fan Speed	100.0%	50.0%
Generate Support	-	Yes
Support Extruder	-	Extruder 2
Support Structure	-	Normal
Support Placement	-	Everywhere
Support Overhang Angle	-	50.0 °
Support Z Distance	-	0.0 mm
Support Horizontal Expansion	-	0.8 mm
Support Interface Thickness	-	0.6 mm
Support Interface Density	-	100.0 %
Support Interface Pattern	-	Zig Zag
Enable Prime Blob	No	No
Build Plate Adhesion Type	Brim	Brim
Build Plate Adhesion Extruder	Not overridden	Not overridden
Enable Prime Tower	Yes	Yes
Prime Tower X Position	294.2 mm	294.2 mm
Prime Tower Y Position	206.2 mm	206.2 mm
Nozzle Switch Retraction Distance	16.0 mm	12.0 mm
Nozzle Switch Retraction Speed	20.0 mm/s	20.0 mm/s